
Parallel Test-Time Scaling with Multi-Sequence Verifiers

Yegon Kim¹ Seungyoo Lee¹ Chaeyun Jang¹ Hyungi Lee¹ Juho Lee¹

Abstract

Parallel test-time scaling, which generates multiple candidate solutions for a single problem, is a powerful technique for improving large language model performance. However, it is hindered by two key bottlenecks: accurately selecting the correct solution from the candidate pool, and the high inference latency from generating many full solutions. We argue that both challenges are fundamentally linked to verifier calibration. A well-calibrated verifier not only improves answer selection, but also enables early-stopping strategies to reduce latency. However, existing verifiers are limited as they score each candidate in isolation, overlooking rich contextual information across the set of candidates. To address this, we introduce the Multi-Sequence Verifier (MSV), the first verifier designed to jointly process all candidate solutions and model their interactions. MSV achieves improved calibration, which directly enhances best-of-N selection performance. We further introduce a streaming MSV variant that empowers a novel early-stopping framework. Our novel framework fully leverages parallel decoding, which contrasts with the existing multi-sequence early exit works that decode sequences one by one and thus incur significant latency. In this novel setting, MSV can achieve the same target accuracy with around half the latency that would be required with its counterpart that scores each solution in isolation.

1. Introduction

Large language models (Brown et al., 2020) have become increasingly powerful, with much of their performance unlocked by test-time scaling strategies. One of the most effective strategies is parallel scaling, where a model generates multiple, independent candidate solutions for a single problem (Wang et al., 2022; Lightman et al., 2023; Snell

et al., 2024). Parallel scaling can be especially fruitful (Snell et al., 2024) when complemented with sequential scaling methods (Wei et al., 2022; Jaech et al., 2024; Guo et al., 2025) that search for and revise solutions adaptively inside a chain of thought. However, parallel scaling faces two bottlenecks that limit its usage: (1) the selection problem, as accurately identifying the correct solution from a large pool of candidates is difficult, and (2) the high inference latency required to generate numerous full solutions.

We argue that these two bottlenecks are not independent; their solutions are deeply connected through the principle of calibration. The selection problem is fundamentally a classification task, where a verifier (Cobbe et al., 2021; Lightman et al., 2023) must accurately estimate the correctness of each solution. Its ability to do so, its calibration (Guo et al., 2017; Kadavath et al., 2022), directly determines the performance of downstream parallel scaling methods such as best-of-N. Concurrently, the high cost of generation can be mitigated by early stopping, a technique that also hinges on a well-calibrated verifier to score intermediate answers and terminate decoding once a threshold score is exceeded (Zhang et al., 2025a; Yang et al., 2025). Although this approach has only been explored in the single-sequence setting, we propose in our paper a way to extend it to parallel scaling. Thus, a verifier with superior calibration is the key to solving both the accuracy and efficiency challenges of parallel scaling.

A fundamental limitation of existing verifiers is their isolated approach to scoring, which overlooks the rich contextual information available across a full set of generated outputs. The success of self-consistency (Wang et al., 2022; Lyu et al., 2025), which relies on the simple cross-sequence statistic of vote counting, serves as a crucial insight: global statistics of sequences can be highly predictive of individual correctness. Yet, this insight has remained surprisingly underexplored. We generalize this principle and introduce the Multi-Sequence Verifier (MSV), the first verifier model designed to learn from the interactions between all candidate solutions. By jointly processing multiple outputs, MSV produces highly accurate and calibrated scores, achieving state-of-the-art performance on standard calibration metrics.

MSV’s superior calibration directly translates into im-

¹Graduate School of AI, KAIST, Seoul, South Korea. Correspondence to: Yegon Kim <yegonkim@kaist.ac.kr>.

proved performance on both the parallel scaling bottlenecks. First, it enhances best-of-N decoding, leading to a more accurate final answer selection and more reliable confidence scores for the chosen answers. Second, and more significantly, we introduce a streaming variant of MSV that empowers a novel framework for early stopping coupled with parallel decoding. We decode multiple sequences in parallel while the streaming MSV calibrates their intermediate answers in real-time by jointly observing all the sequences. Decoding terminates the moment that the confidence of any one sequence exceeds a threshold.

To be concrete, our experiments show that on challenging math reasoning benchmarks, MSV improves best-of-64 accuracy by over 6% relative to strong weighted-voting baselines. This accuracy gain is accompanied by a dramatic improvement in the calibration of the selected answer’s confidence score, with MSV reducing the Expected Calibration Error by over 75%. The benefits are even more notable in our parallel early-stopping framework, where our streaming MSV achieves the same peak accuracy as baseline verifier models with as little as half the latency. These downstream improvements stem directly from MSV’s superior calibration, evidenced for instance by a 50% reduction in the Brier score compared to baseline models that score sequences in isolation.

Our contributions can be summarized as follows:

- We propose the Multi-Sequence Verifier (MSV), a novel verifier architecture that models cross-sequence interactions to achieve improved calibration.
- We demonstrate that improved calibration from MSV directly translates to enhanced best-of-N answer selection and more calibrated confidence levels associated with the chosen answers.
- We generalize an existing early-stopping framework to the parallel decoding setting, and introduce a streaming MSV variant that outperforms strong baselines in this novel setting.

2. Related Work

2.1. Calibration of LLM Outputs

Confidence estimation for LLMs has been studied through black-box and white-box approaches. Black-box approaches have focused on prompting a language model to verbalize its confidence (Lin et al., 2022; Tian et al., 2023). Xiong et al. (2023) finds that white-box approaches to calibration, which instead probe internal states (Kadavath et al., 2022), generally outperform their black-box counterparts. Lyu et al. (2025) investigates using global sequence statistics such as the entropy of answer distribution to calibrate the majority voted answer, but their method cannot be applied to calibrating the other answers. Zhang et al.

(2025a) demonstrates an interesting result that intermediate answers from reasoning models such as DeepSeek R1 (Guo et al., 2025) can be robustly calibrated through lightweight probes on their hidden states, and apply this finding to early stopping in the decoding of a single sequence.

2.2. Parallel Test-Time Scaling

Answer selection among multiple decoded sequences is a crucial component of parallel test-time scaling. One can regard this task as well-calibrated ranking of answers within a problem such that the correct answers are scored higher than the incorrect ones. As such, the most common approach is to train calibrated verifier models (Cobbe et al., 2021; Zhang et al., 2024). Self-consistency (Wang et al., 2022) is a simple selection method that doesn’t require training of a verifier model, and instead selects the answer with the most numerous occurrence among sequences. This hints at the possible usefulness of global statistics, or in other words looking at multiple sequences together, in improved calibration and answer selection. Tangentially related is multi-agent debate (Du et al., 2023), since debate with a single round is equivalent to best-of-N selection with critics that look at all the generated sequences. Again, the effectiveness of debate hints at the usefulness of cross-sequence features in estimating individual correctness. We note that most research in parallel test-time scaling, including ours, makes a minimal assumption that there is a symbolic checker, e.g. SymPy (Meurer et al., 2017), that evaluates the equivalence between two answers.

2.3. Adaptive Scaling for Efficiency

The efficiency of parallel test-time scaling is essential for its practical usage. Most works on efficient test-time scaling focus on adaptively scaling the test-time compute, for instance by refraining from sampling more sequences when all the previous sequences agree with each other in their answers. However, they largely disregard the tradeoff between latency and throughput. It is desirable, in practical settings, to reduce latency by acquiring a larger throughput, even if the total amount of test-time computation remains the same. Various works such as DeepConf (Fu et al., 2025) and others (Li et al., 2024; Aggarwal et al., 2023; Xue et al., 2023; Huang et al., 2025) propose early stopping at the sequence level to reduce the number of decoded sequences. However, they all assume multiple sequences being decoded sequentially, and as a result, incur tens to hundreds of times the latency of a single sequence, limiting their practical usage. We instead focus on parallel decoding with token-level early stopping. To the best of our knowledge, we are the first in the LLM decoding literature to investigate this setting. Our paper aims at improving over simple but strong baselines in this novel setting.

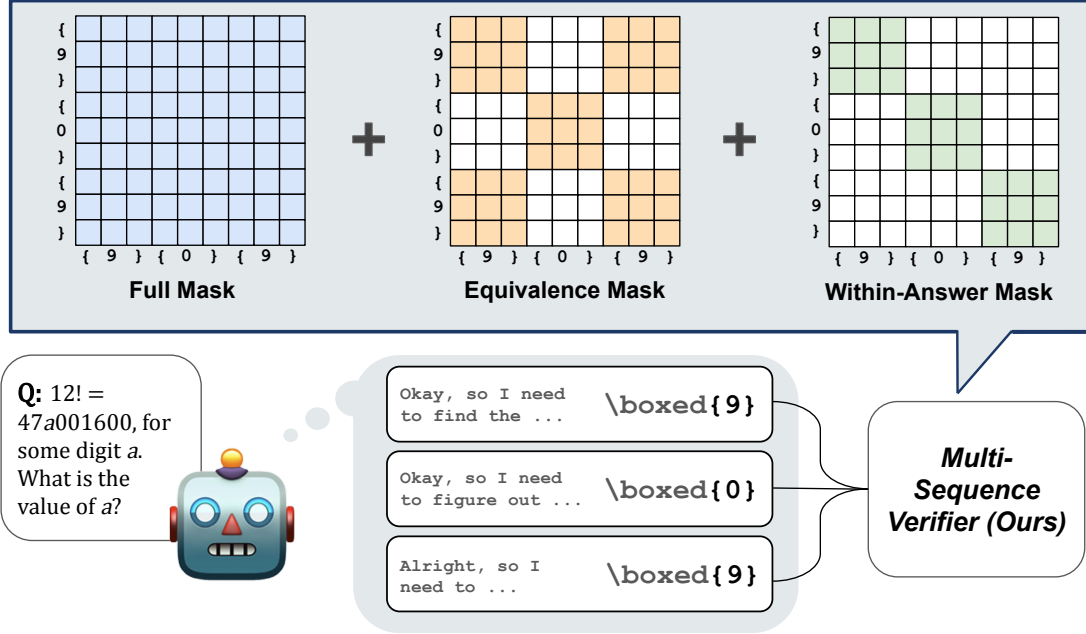


Figure 1. Illustration of our Multi-Sequence-Verifier (MSV) that uses multiple attention masks in its Multi-Mask Transformer Block (MMTB) to predict the correctness of each answer. The different attention masks allow MSV to flexibly leverage information both across and within sequences.

3. Method

3.1. Problem Setup

In this paper, we assume a *parallel decoding* or *parallel sampling* scenario, where our LLM model generates N sequences simultaneously for a given query q . At each decoding step, one token is sampled for every sequence, in parallel. This parallel approach reduces latency compared to sequential decoding, a crucial advantage for practical applications. Under this scenario, we consider two settings: 1) **Terminal Answers** and 2) **Streaming Answers**. In brief, the **Terminal Answers** setting focuses on the final answers obtained from each sequence after decoding has been complete. The **Streaming Answers** setting additionally focuses on the intermediate answers produced while decoding. We describe each setting in more detail below.

Terminal Answers. Given a query q , the LLM decodes N parallel sequences until they all reach termination. To extract an explicit answer, we append an elicitation prompt such as `### Final Answer ### \boxed` to the end of each n th sequence, prompting the model to produce a boxed answer $a^{(n)}$. This results in one answer per sequence, denoted by $\{a^{(n)}\}_{n=1}^N$.

Streaming Answers. Unlike the **Terminal Answers** setting, we additionally extract *intermediate answers* whenever a delimiter, e.g., the token “Wait”, is encountered. This approach of extracting intermediate answers at delimiters has been explored in prior work for single-

sequence early stopping (Zhang et al., 2025a; Yang et al., 2025), which we generalize to the parallel decoding setting with multiple sequences. Specifically, when the k th delimiter appears in the n th sequence, we immediately branch that sequence, append the elicitation prompt `### Final Answer ### \boxed`, and obtain an intermediate answer $a_k^{(n)}$. We also extract the terminal answer at the end of each sequence. Thus, if a sequence contains $K^{(n)} - 1$ delimiters, it may yield multiple answers $\{a_k^{(n)}\}_{k=1}^{K^{(n)}}$, where $a_{K^{(n)}}^{(n)}$ is the terminal answer. For notational consistency, in the **Terminal Answers** setting, we regard the single terminal answer as $a_1^{(n)}$ and $K^{(n)} = 1$.

Along with each answer, we store the representations of the answer tokens for later use with our Multi-Sequence Verifier. Specifically, if $a_k^{(n)}$ consists of $L_k^{(n)}$ tokens, we store $\{h_{k,i}^{(n)}\}$ for $i = 1, \dots, L_k^{(n)}$, where $h_{k,i}^{(n)} \in \mathbb{R}^d$ denotes the d -dimensional hidden state of the i th token, output by the last transformer layer of the LLM.

Correctness and learning objectives. Now, we define the correctness of an answer $a_k^{(n)}$ generated from a sequence. Let a^* denote the ground-truth answer for the query q , and the symbol \sim be an equivalence relation that captures symbolic or semantic equality, e.g., “ $2 + 2$ ” \sim “ 4 ”, that can be computed with an algorithm such as SymPy (Meurer et al., 2017; Lewkowycz et al., 2022). Then, we define the correctness of each candidate answer $a_k^{(n)}$ as follows:

$$y_k^{(n)} = \mathbf{1} [a_k^{(n)} \sim a^*].$$

Our goal is to accurately predict $y_k^{(n)}$ for every candidate, so that we can make more effective use of the generated answers in downstream parallel test-time scaling methods such as best-of-N.

Departing from methods that classify each answer in isolation, we propose to *leverage information across multiple sequences* to further improve the predictions. Specifically, in the **Terminal Answers** setting, the prediction for $a_1^{(i)}$ may depend on the entire set of terminal answers $\{a_1^{(n)}\}_{n=1}^N$. In contrast, in the **Streaming Answers** setting, the predictors must respect causality: the correctness prediction for $a_k^{(n)}$ may only use information from tokens generated *up to that point in time* across all sequences. A detailed description of our method is provided below.

3.2. Multi-Sequence Verifier

In this section, we present our novel verifier architecture, MSV. The verifier predicts the correctness of each answer by consuming that answer tokens’ (last-layer) hidden states and *aggregating* auxiliary signals drawn from the answers produced by the other sequences. This cross-sequence aggregation enables MSV to judge the correctness of a single answer in the context of peer outputs, leading to better-calibrated predictions than when relying on information from a single answer alone. See Figure 1 for a schematic diagram of MSV, and Algorithm 1 for a pseudocode of MSV’s forward pass.

Input representation for MSV. Let t be a time index shared across parallel sequences, where all the sequences start generating from $t = 0$ and they generate one token at a time. Let $\tau_k^{(n)}$ denote the time stamp at which the n th sequence generates the k th answer $a_k^{(n)}$. At a specific readout time step t , MSV takes the representations of all the answers generated up to the step t to predict the correctness of the answers. Specifically, we collect the representations as follows,

$$U^{(t)} = \text{concat} \left(\left\{ \left\{ \left\{ h_{k,i}^{(n)} + e^{(n)} \right\}_{i=1}^{L_k^{(n)}} \right\}_{\tau_k^{(n)} \leq t} \right\}_{n=1}^N \right).$$

Here, $\text{concat}(\cdot)$ denotes concatenation of all the representations along the sequence dimension, without adding any special separators between sequences. $e^{(n)}$ is a learnable per-sequence embedding added to identify the sequence from which each token representation originates.

Multi-mask transformer blocks. To process the aggregated representation $U^{(t)}$, we introduce a **Multi-Mask Transformer Block (MMTB)**. This block captures diverse aspects of the token sequences by combining multiple attention outputs, each derived from a different mask applied to the same input, $U^{(t)}$. As in standard multi-head attention (Vaswani et al., 2017), we begin by computing the

usual linear projections of $U^{(t)}$ into query, key, and value matrices $(Q_h^{(t)}, K_h^{(t)}, V_h^{(t)})_{h=1}^H$ where H is the number of heads. For a fixed collection of J masks $\{M_j\}_{j=1}^J$, we then compute the output for each mask:

$$A_{h,j}^{(t)} = \text{softmax} \left(\frac{Q_h^{(t)} (K_h^{(t)})^\top}{\sqrt{d}} + \log M_j \right) V_h^{(t)},$$

where $\log M_j$ adds 0 to permitted entries and $-\infty$ to masked entries, with softmax applied row-wise. The masked outputs are then combined via learnable mixture weights $\mathbf{w}_h = (w_{h,1}, \dots, w_{h,J})$ for each head h :

$$\tilde{U}^{(t)} = \sum_{h=1}^H \sum_{j=1}^J \alpha_{h,j} A_{h,j}^{(t)}, \quad \alpha_h = \text{softmax}(\mathbf{w}_h).$$

The collection of masks $\{M_j\}_{j=1}^J$ is a fixed hyperparameter of our model. In our instantiation, we use four complementary masks. The *full* mask permits all interactions, $(M_{\text{full}})_{u,v} = 1$ for all positions u, v , enabling attention across all tokens in all sequences. The *within-sequence* mask restricts attention to tokens originating from the same sequence,

$$(M_{\text{ws}})_{u,v} = \mathbf{1}[\text{seq}(u) = \text{seq}(v)],$$

capturing within-sequence signals while blocking cross-sequence signals. Here, $\text{seq}(u)$ denotes the index n of the sequence containing the token u . The *equivalence* mask allows attention only between tokens whose answers are symbolically equivalent,

$$(M_{\text{eq}})_{u,v} = \mathbf{1}[\text{ans}(u) \sim \text{ans}(v)],$$

where $\text{ans}(u)$ is the answer $a_k^{(n)}$ containing the token u .

Finally, the *within-answer* mask allows attention only between tokens inside a single answer instance $a_k^{(n)}$,

$$(M_{\text{wa}})_{u,v} = \mathbf{1}[(\text{seq}(u), \text{step}(u)) = (\text{seq}(v), \text{step}(v))],$$

where $\text{step}(u)$ identifies the answer step k to which the token belongs.

To summarize, $a_k^{(n)}$ can attend to $a_{k'}^{(n')}$ (1) through the full mask, (2) through the within-sequence mask if $n = n'$, (3) through the equivalence mask if $a_k^{(n)} \sim a_{k'}^{(n')}$, and (4) through the within-answer mask if $n = n'$ and $k = k'$. In the **Terminal Answers** setting, the within-sequence mask and within-answer mask are equivalent, reducing the number of masks to three. We further restrict the attention masks to be “causal” in the **Streaming Answers** setting, meaning that an answer $a_k^{(n)}$ may attend to $a_{k'}^{(n')}$ only if $\tau_k^{(n)} \geq \tau_{k'}^{(n')}$. We provide an ablation study of each mask, in Section B.3.

The block’s final output is then computed using standard residual connections and an MLP layer:

$$Z^{(t)} = (U^{(t)} + \tilde{U}^{(t)}) + \text{MLP}(\text{LN}(U^{(t)} + \tilde{U}^{(t)})),$$

Here, MLP denotes a Multi-Layer Perceptron and LN is layer normalization, consistent with the standard self-attention plus MLP architecture.

Feature augmentation. While the aggregated representation $Z^{(t)}$ has undergone the MMTB module which updates token representations by modeling relationships across sequences, we further enrich each answer’s representation with an explicit statistic: the proportion of sequences that produce symbolically equivalent answers. Although attention over all tokens could, in principle, internalize such counting signals, exact counting is known to be challenging for Transformer architectures (Barbero et al., 2024; Ouellette et al., 2023). Motivated by this, we compute the fraction $\gamma_k^{(n)} \in [0, 1]$ of sequences whose answers are equivalent to $a_k^{(n)}$, and inject it as a learned feature by projecting it through a small MLP which is then added to the hidden states. Specifically, from $Z^{(t)}$, we extract the representation $z_{k,L_k}^{(n)}$ corresponding to the last token of $a_k^{(n)}$, and add the information from $\gamma_k^{(n)}$, as follows:

$$\tilde{z}_k^{(n)} = z_{k,L_k}^{(n)} + \text{MLP}(\gamma_k^{(n)}).$$

We only use the last token representation $z_{k,L_k}^{(n)}$ for computing the prediction, because the attention layer in MMTB has already aggregated the relevant information from all the other tokens in $a_k^{(n)}$.

Constructing final predictions. To predict the final correctness of $a_k^{(n)}$, we apply a linear head to its augmented representation and pass the resulting logit through a sigmoid:

$$\tilde{y}_k^{(n)} = \sigma(\mathbf{w}^\top \tilde{z}_k^{(n)} + b),$$

where σ denotes the sigmoid function and \mathbf{w}, b are learnable parameters. Additionally, in the **Terminal Answers** setting, instead of computing each $\tilde{y}_1^{(n)}$ independently, we first average the *logits* of symbolically equivalent terminal answers and then apply the sigmoid function as follows,

$$\tilde{y}_1^{(n)} = \sigma\left(\frac{1}{|\mathcal{C}(n)|} \sum_{m \in \mathcal{C}(n)} (\mathbf{w}^\top \tilde{z}_1^{(m)} + b)\right)$$

where $\mathcal{C}(n) := \{m \in \{1, \dots, N\} \mid a_1^{(m)} \sim a_1^{(n)}\}$. Logit averaging incorporates our a priori knowledge that symbolically equivalent answers share the same correctness label. Logit averaging is inappropriate in the case of **Streaming Answers**, because the information carried by $\tilde{z}_k^{(n)}$ grows with k , and logits at earlier steps might disrupt rather than complement the prediction at the current step k .

Training and Inference. For the **Streaming Answers** scenario, we run the sequences until all of them terminate, collect all the intermediate and final answers produced, and train the parameters to minimize the binary cross-entropy loss. Let T be the global time step when all the sequences terminate. We first compute $Z^{(T)}$, compute the predictions $\tilde{y}_k^{(n)}$, and minimize

$$\mathcal{L} := \sum_{n,k} \text{BCE}(\tilde{y}_k^{(n)}, y_k^{(n)}),$$

where the summation is over all valid n, k pairs. For the **Terminal Answers** scenario, we proceed similarly, except that we minimize BCE only for the terminal answers. BCE is a strictly proper loss, which incentivizes calibrated probabilities under standard assumptions. (Blasiok et al., 2023)

At inference time, whenever we want to predict whether the sequences are producing correct answers at some specific time t , we compute $Z^{(t)}$, and predict $\{\{\tilde{y}_k^{(n)}\}_{\tau_k^{(n)} \leq t}\}_{n=1}^N$.

3.3. Applications

In this section, we present how to use the MSV-based correctness predictions $\tilde{y}_k^{(n)}$ in the **Terminal Answers** and **Streaming Answers** settings. Basically, in the **Terminal Answers** setting, we use $\tilde{y}_1^{(n)}$ as a verifier score for *best-of- N* selection, whereas in the **Streaming Answers** setting, we use $\tilde{y}_k^{(n)}$ both as an early-stopping signal and as a criterion for selecting the best candidate. Detailed descriptions are provided below.

Calibrated best-of- N predictions. In the **Terminal Answers** scenario, our verifier scores are used for *best-of- N* decoding, a robust technique for improving performance (Nakano et al., 2021). From N candidate answers, we select the one, a^\dagger , with the highest score:

$$n^\dagger = \arg \max_n \tilde{y}_1^{(n)}, \quad a^\dagger = a_1^{(n^\dagger)}.$$

A key advantage of this approach is that the score for the chosen answer, $\tilde{y}^\dagger = \tilde{y}_1^{(n^\dagger)}$, is also a calibrated confidence estimate of a^\dagger being correct (Guo et al., 2017). This allows us to assess not only *which* answer is best but also *how likely* it is to be correct.

Early stopping of parallel decoding. In the **Streaming Answers** setting, multiple sequences are decoded in parallel, and each intermediate answer $a_k^{(n)}$ yields a correctness score $\tilde{y}_k^{(n)}$. We define an early-stopping rule that halts decoding once the best available candidate exceeds a threshold λ :

$$t^* = \min \left\{ t : \max_{n,k: \tau_k^{(n)} \leq t} \tilde{y}_k^{(n)} \geq \lambda \right\}.$$

At t^* , we output the candidate with the highest predicted score, which is the candidate that caused the early-stopping. If the system terminates without any of the decoded answers exceeding the threshold, the system outputs the best among the final answers $\tilde{y}_{K^{(n)}}^{(n)}$:

$$n^\dagger = \arg \max_n \tilde{y}_{K^{(n)}}^{(n)}, \quad a^\dagger = a_{K^{(n)}}^{(n)}.$$

Thus, $\tilde{y}_k^{(n)}$ acts both as the stopping signal and as verifier scores for selecting the best answer.

4. Experiments

4.1. Experimental Setup

In this section, we present empirical evidence that demonstrates the effectiveness of MSV, our novel verifier that leverages information across all sequences. We denote MSV trained on groups of N sequences, by MSV_N . For strong baselines that classify each sequence in isolation, or *single-sequence baselines* for short, we consider two methods: 1) “ MSV_1 ”, trained only on each sequence, and 2) “Probe” (Zhang et al., 2025a), which trains an MLP on last-token representations to predict the correctness of each answer. Although we can directly use these two methods as verifiers in the multiple-sequence setting, both are single-sequence predictors and hence can be complemented by aggregation methods that combine verifier scores across sequences. To this end, we adopt a strong aggregation method called Weighted Voting (WV; Li et al., 2022), which aggregates correctness probabilities by summing them within each class of equivalent answers and normalizing across classes, extending the single-sequence baselines for a fair comparison with MSV_N . In the experiments, this extension is denoted as $A+\text{WV}$, where A represents either Probe or MSV_1 . We also present results with self-consistency and the open-source verifier Qwen2.5-Math-PRM-7B (Zhang et al., 2025b), in Section D.3 and Section B.9, respectively. Both methods far underperform other baselines that we do present in this section. We assess calibration with AUROC, Expected Calibration Error (ECE; Naeini et al., 2015), and the Brier Score (BS; Brier, 1950), where higher AUROC and lower ECE/BS indicate better performance. Details on the metrics are provided in Section A.

We use the DeepSeek-R1-Distill-Qwen-1.5B model (Guo et al., 2025) as the base LLM. Experiments with three other base LLMs can be found in Section B.5. DeepMath-103K (He et al., 2025) is used for training and validation, and evaluation is conducted on MATH (Hendrycks et al., 2021), OlympiadBench (OB; He et al., 2024), AMC12, AIME, and Omni-MATH (OM; Gao et al., 2024) datasets. All experiments are done on five random seed values. We provide further details of the experimental setup in Sec-

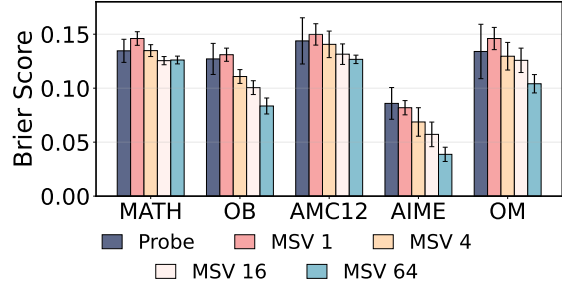


Figure 2. Brier scores (\downarrow) of baselines and MSV_N in the **Terminal Answers** setting. OB refers to OlympiadBench, and OM refers to Omni-MATH. Full results are in Table 23.

tion A, along with a report of all experiments in Section D.

4.2. Terminal Answers setting

In this section, we conduct experiments in the **Terminal Answers** setting. We first demonstrate, empirically, that MSV_N predicts the correctness of each candidate answer more accurately than baseline methods, as evidenced by their improvements on the standard calibration metrics. We then show that, in the *best-of- N* scenario, using MSV_N as a verifier results in better accuracy and calibration of the chosen answer, compared to the baselines.

Calibration on Terminal Answers. Calibration of verifiers is presumably the key determinant of effective parallel scaling. We measure the average calibration performance of the verifier models. Figure 2 reports the Brier score of single-sequence baselines and MSV_N on the five evaluation sets. We find that MSV_N consistently achieves better calibration compared to all baselines, and that the performance scales reliably as N increases. On the AIME dataset, MSV_{64} achieves a $\sim 50\%$ reduction in BS compared to Probe. Our results clearly demonstrate that leveraging information across multiple sequences can indeed be used to improve the calibration of verifiers.

Calibrated best-of- N Prediction. We apply MSV_N , our superior verifier model that leverages cross-sequence attention, to best-of- N answer selection and its associated confidence output. As shown in Figure 3, MSV_N consistently improves best-of- N accuracy over all baselines, with gains becoming more pronounced as N increases. At $N = 64$, MSV_{64} achieves a $\sim 6\%$ improvement over the strongest single-sequence baselines, across all datasets. Moreover, MSV_N keeps improving with growing N , while the baselines often plateau or even deteriorate, consistent with the observation in Snell et al. (2024). Table 32 reports the accuracy of self-consistency and other verifier-free methods, which all underperform significantly compared to our verifier baselines and MSV_N .

Given that the weighted voting (WV) methods achieve the

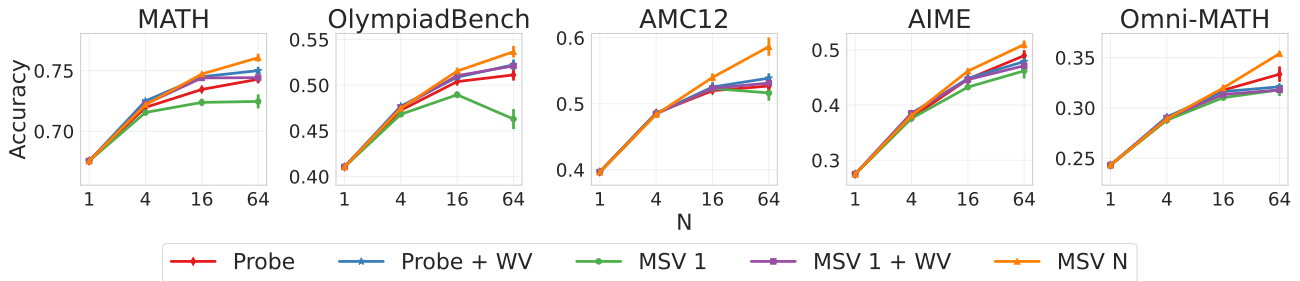


Figure 3. Best-of- N accuracy vs. N , in **Terminal Answers** setting. Full results are in Table 25.

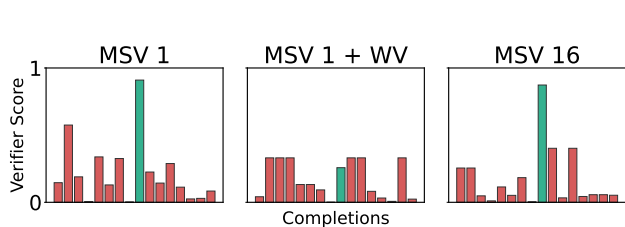


Figure 4. Probability estimates for a single problem with 16 completions, comparing MSV_1 , MSV_1+WV , and MSV_{16} .

Table 1. ECE of confidence output by verifiers on their *best-of-64 answers*. A lower ECE implies better calibration. Full results are in Table 26.

Method	MATH	AIME	OM
Probe	0.185 \pm 0.028	0.301 \pm 0.059	0.419 \pm 0.080
MSV_1	0.213 \pm 0.014	0.316 \pm 0.035	0.450 \pm 0.030
MSV_{64}	0.132 \pm 0.015	0.075 \pm 0.050	0.130 \pm 0.027

performance closest to that of MSV_N , one might hypothesize that the behavior of MSV_N is similar to WV, lifting the score of answers that appear frequently while suppressing answers that appear scantily. Figure 4 shows the predictions of MSV_1 , MSV_1+WV , and MSV_{16} on a problem with one correct sequence, marked by green. Contrary to the hypothesis, MSV_{16} behaves in a starkly different manner from WV, which incorrectly suppresses the correct answer due to its low voting count of one.

Beyond obtaining the correct answer on a problem, outputting a calibrated confidence level on the chosen answer is crucial in risk-sensitive settings, where reliable certainty is required to make trustworthy, high-stakes decisions. ECE is a metric directly relevant to trustworthiness, as it measures how well the confidence levels align with the true rates of correctness. Table 1 shows that MSV_{64} consistently lowers the best-of- N answer ECE across all datasets, most notably reducing it to just 25% of Probe on AIME. Reliability diagrams (Sanders, 1963; Guo et al., 2017) in Figure 5 further confirm that MSV_{64} outputs more diverse and well-aligned confidence estimates, and additional metrics in Table 26 indicate similar improvements.

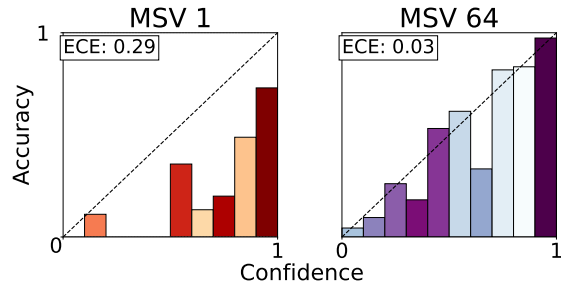


Figure 5. Reliability diagrams of verifier confidence on best-of-64 answers (AIME).

In summary, modeling cross-sequence interactions with MSV_N not only boosts best-of- N accuracy, but also delivers substantially more reliable confidence estimates, strengthening its utility for downstream decision-making.

4.3. Streaming Answers

In this section, we conduct experiments in the **Streaming Answers** setting. Unlike **Terminal Answers**, this setting involves early stopping, and thus accurately predicting the correctness of intermediate answers is directly tied to both performance and efficiency. We first examine how much MSV_N improves calibration on intermediate answers, and then empirically validate how this improved calibration contributes to the effectiveness of early stopping. We use the “Wait” token as the delimiter throughout this section, but experiments with two other delimiters in Section B.8 show that the trends are insensitive to the choice.

Calibration on Streaming Answers. Table 2 provides the Brier scores of verifiers on intermediate answers. We see that MSV_{64} significantly improves calibration, lowering the Brier score on AIME by more than half compared to Probe. A full report with other choices of N and evaluation sets can be found in Table 27. Figure 7 plots the BS calculated per bins of intermediate answers in fine-grained ranges of token positions. We see that MSV_{64} improves over baselines at every range, without exception. Furthermore, the gap in performance tends to increase for answers that appear later in the sequences.

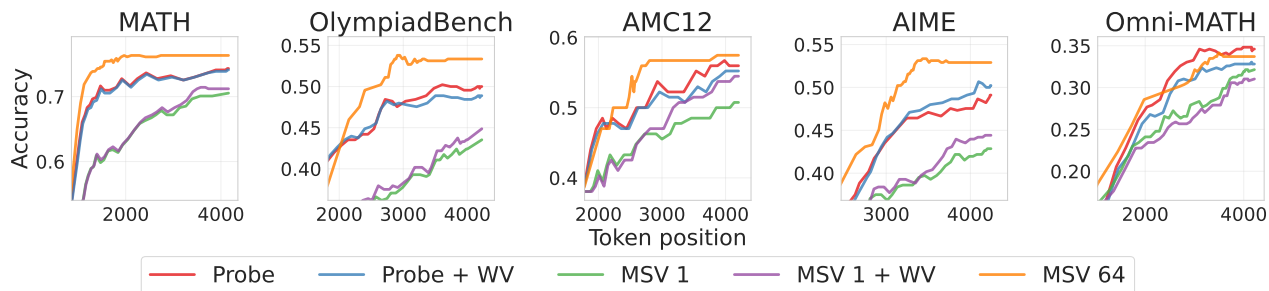


Figure 6. Accuracy-latency tradeoff curves in **Streaming Answers**, with $N = 64$. Curves that lie higher above are superior in that they require lower latency to achieve the same accuracy. Full results are in Table 29. Wall-clock latency are in Section B.1.

Table 2. Brier score of verifiers trained and evaluated in **Streaming Answers**. Full results are in Table 27.

Method	MATH	AIME	OM
Probe	0.159 \pm 0.010	0.080 \pm 0.011	0.153 \pm 0.024
MSV ₁	0.160 \pm 0.013	0.064 \pm 0.003	0.138 \pm 0.008
MSV ₆₄	0.115 \pm 0.002	0.032 \pm 0.001	0.126 \pm 0.005

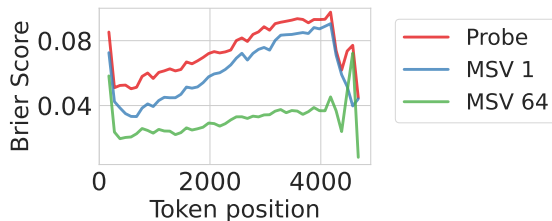


Figure 7. Brier score of verifiers per token position, on AIME.

Parallel early-stopping. Next, we investigate whether the superior calibration on intermediate answers can indeed transfer to improved performance in parallel early stopping that was introduced in Section 3.3. We compare MSV_N with the single-sequence baselines, including the WV methods. In Section A.1, we describe how WV is implemented in the Streaming Answers setting. Recall that early stopping is done with some threshold value $0 \leq \lambda \leq 1$. At each threshold λ , we can plot the average accuracy of the early stopped answers, and the average latency, which we approximate with the early stopped token positions. Therefore, sliding λ between 0 and 1 creates an accuracy-latency tradeoff curve for each verifier.

In Figure 6, we plot the accuracy-latency tradeoff curves of MSV_1 , MSV_1+WV , and MSV_{64} , when performing early stopping with $N = 64$ parallel sequences. We observe significant improvement of MSV_{64} over the single sequence baselines. On the MATH dataset, we find that the maximum achievable accuracy with single-sequence baselines can be achieved by MSV_{64} with less than half the latency. The actual wall-clock latency measurements can be found in Section B.1, which shows that the overheads incurred by verifier inference and intermediate answer generation are minimal.

Both the best-of-N results in **Terminal Answers** and the parallel early stopping results in **Streaming Answers** support our hypothesis that improved calibration of verifiers effectively transfer to their downstream performance in parallel scaling methods.

5. Conclusion

In this work, we addressed two critical bottlenecks in the parallel test-time scaling of large language models: the accurate selection of correct solutions and the high inference latency from generating multiple candidates. We argued that both challenges are fundamentally linked to verifier calibration and that existing verifiers are limited by scoring candidate solutions in isolation. To overcome this, we introduced the Multi-Sequence Verifier (MSV), a novel architecture designed to jointly process an entire set of candidate solutions and model their interactions. Our extensive experiments demonstrated that MSV achieves state-of-the-art calibration, significantly outperforming strong baselines that score sequences independently. This improved calibration directly translated to substantial downstream benefits. For best-of-N decoding, MSV improved selection accuracy by over 6% and reduced the Expected Calibration Error of the final chosen answers by over 75%.

Furthermore, we introduced a novel parallel early-stopping framework for efficient inference that contrasts with prior sequential approaches. In this framework, a streaming variant of MSV achieved the same peak accuracy as baseline verifiers with around half the latency. These findings underscore the importance of cross-sequence information and establish a new, more effective approach to building and utilizing verifiers for parallel scaling.

Impact Statement.

We propose a new method that improves calibration of verifiers for improved downstream parallel scaling performance. Although our approach doesn't have a direct positive or negative impact in ethical or societal aspects, it improves and accelerates task completions with LLMs through parallel scaling. This could be used for good, such as reliable decision-making in problems that benefit the society. However, like many technologies, this method could also be misused in domains where improved decision-making can be used with bad intentions. Therefore, researchers and practitioners should apply these methods with consideration of their broader societal implications, aiming to ensure that the benefits of the technology are used responsibly and ethically.

References

- Aggarwal, P., Madaan, A., Yang, Y., et al. Let's sample step by step: Adaptive-consistency for efficient reasoning and coding with llms. *arXiv preprint arXiv:2305.11860*, 2023.
- Barbero, F., Banino, A., Kapturowski, S., Kumaran, D., Madeira Araújo, J., Vitvitskiy, O., Pascanu, R., and Veličković, P. Transformers need glasses! information over-squashing in language tasks. *Advances in Neural Information Processing Systems*, 37:98111–98142, 2024.
- Blasiok, J., Gopalan, P., Hu, L., and Nakkiran, P. When does optimizing a proper loss yield calibration? *Advances in Neural Information Processing Systems*, 36:72071–72095, 2023.
- Brier, G. W. Verification of forecasts expressed in terms of probability. *Monthly weather review*, 78(1):1–3, 1950.
- Brown, T., Mann, B., Ryder, N., Subbiah, M., Kaplan, J. D., Dhariwal, P., Neelakantan, A., Shyam, P., Sastry, G., Askell, A., et al. Language models are few-shot learners. *Advances in neural information processing systems*, 33:1877–1901, 2020.
- Cobbe, K., Kosaraju, V., Bavarian, M., Chen, M., Jun, H., Kaiser, L., Plappert, M., Tworek, J., Hilton, J., Nakano, R., et al. Training verifiers to solve math word problems. *arXiv preprint arXiv:2110.14168*, 2021.
- Du, Y., Li, S., Torralba, A., Tenenbaum, J. B., and Mordatch, I. Improving factuality and reasoning in language models through multiagent debate. In *Forty-first International Conference on Machine Learning*, 2023.
- Fu, Y., Wang, X., Tian, Y., and Zhao, J. Deep think with confidence. *arXiv preprint arXiv:2508.15260*, 2025.
- Gao, B., Song, F., Yang, Z., Cai, Z., Miao, Y., Dong, Q., Li, L., Ma, C., Chen, L., Xu, R., et al. Omni-math: A universal olympiad level mathematic benchmark for large language models. *arXiv preprint arXiv:2410.07985*, 2024.
- Guo, C., Pleiss, G., Sun, Y., and Weinberger, K. Q. On calibration of modern neural networks. In *International conference on machine learning*, pp. 1321–1330. PMLR, 2017.
- Guo, D., Yang, D., Zhang, H., Song, J., Zhang, R., Xu, R., Zhu, Q., Ma, S., Wang, P., Bi, X., et al. Deepseek-r1: Incentivizing reasoning capability in llms via reinforcement learning. *arXiv preprint arXiv:2501.12948*, 2025.
- He, C., Luo, R., Bai, Y., Hu, S., Thai, Z. L., Shen, J., Hu, J., Han, X., Huang, Y., Zhang, Y., et al. Olympiadbench: A challenging benchmark for promoting agi with olympiad-level bilingual multimodal scientific problems. *arXiv preprint arXiv:2402.14008*, 2024.
- He, Z., Liang, T., Xu, J., Liu, Q., Chen, X., Wang, Y., Song, L., Yu, D., Liang, Z., Wang, W., et al. Deepmath-103k: A large-scale, challenging, decontaminated, and verifiable mathematical dataset for advancing reasoning. *arXiv preprint arXiv:2504.11456*, 2025.
- Hendrycks, D., Burns, C., Kadavath, S., Arora, A., Basart, S., Tang, E., Song, D., and Steinhardt, J. Measuring mathematical problem solving with the math dataset. *arXiv preprint arXiv:2103.03874*, 2021.
- Huang, C., Huang, L., Leng, J., Liu, J., and Huang, J. Efficient test-time scaling via self-calibration. *arXiv preprint arXiv:2503.00031*, 2025.
- Jaech, A., Kalai, A., Lerer, A., Richardson, A., El-Kishky, A., Low, A., Helyar, A., Madry, A., Beutel, A., Carney, A., et al. Openai o1 system card. *arXiv preprint arXiv:2412.16720*, 2024.
- Kadavath, S., Conerly, T., Askell, A., Henighan, T., Drain, D., Perez, E., Schiefer, N., Hatfield-Dodds, Z., Das-Sarma, N., Tran-Johnson, E., et al. Language models (mostly) know what they know. *arXiv preprint arXiv:2207.05221*, 2022.
- Lewkowycz, A., Andreassen, A., Dohan, D., Dyer, E., Michalewski, H., Ramasesh, V., Slone, A., Anil, C., Schlag, I., Gutman-Solo, T., et al. Solving quantitative reasoning problems with language models, 2022. [URL https://arxiv.org/abs/2206.14858](https://arxiv.org/abs/2206.14858), 1, 2022.
- Li, Y., Lin, Z., Zhang, S., Fu, Q., Chen, B., Lou, J.-G., and Chen, W. Making large language models better reasoners with step-aware verifier. *arXiv preprint arXiv:2206.02336*, 2022.

- Li, Y., Yuan, P., Feng, S., Pan, B., Wang, X., Sun, B., Wang, H., and Li, K. Escape sky-high cost: Early-stopping self-consistency for multi-step reasoning. *arXiv preprint arXiv:2401.10480*, 2024.
- Lightman, H., Kosaraju, V., Burda, Y., Edwards, H., Baker, B., Lee, T., Leike, J., Schulman, J., Sutskever, I., and Cobbe, K. Let’s verify step by step. In *The Twelfth International Conference on Learning Representations*, 2023.
- Lin, S., Hilton, J., and Evans, O. Teaching models to express their uncertainty in words. *arXiv preprint arXiv:2205.14334*, 2022.
- Liu, R., Gao, J., Zhao, J., Zhang, K., Li, X., Qi, B., Ouyang, W., and Zhou, B. Can 1b llm surpass 405b llm? rethinking compute-optimal test-time scaling. *arXiv preprint arXiv:2502.06703*, 2025.
- Lyu, Q., Shridhar, K., Malaviya, C., Zhang, L., Elazar, Y., Tandon, N., Apidianaki, M., Sachan, M., and Callison-Burch, C. Calibrating large language models with sample consistency. In *Proceedings of the AAAI Conference on Artificial Intelligence*, volume 39, pp. 19260–19268, 2025.
- Meurer, A., Smith, C. P., Paprocki, M., Čertík, O., Kirpichev, S. B., Rocklin, M., Kumar, A., Ivanov, S., Moore, J. K., Singh, S., et al. Sympy: symbolic computing in python. *PeerJ Computer Science*, 3:e103, 2017.
- Naeini, M. P., Cooper, G., and Hauskrecht, M. Obtaining well calibrated probabilities using bayesian binning. In *Proceedings of the AAAI conference on artificial intelligence*, volume 29, 2015.
- Nakano, R., Hilton, J., Balaji, S., Wu, J., Ouyang, L., Kim, C., Hesse, C., Jain, S., Kosaraju, V., Saunders, W., et al. Webgpt: Browser-assisted question-answering with human feedback. *arXiv preprint arXiv:2112.09332*, 2021.
- Ouellette, S., Pfister, R., and Jud, H. Counting and algorithmic generalization with transformers. *arXiv preprint arXiv:2310.08661*, 2023.
- Rodionov, G., Garipov, R., Shutova, A., Yakushev, G., Schultheis, E., Egiazarian, V., Sinitsin, A., Kuznedelev, D., and Alistarh, D. Hogwild! inference: Parallel llm generation via concurrent attention. *arXiv preprint arXiv:2504.06261*, 2025.
- Sanders, F. On subjective probability forecasting. *Journal of Applied Meteorology and Climatology*, 2(2):191–201, 1963.
- Snell, C., Lee, J., Xu, K., and Kumar, A. Scaling llm test-time compute optimally can be more effective than scaling model parameters. *arXiv preprint arXiv:2408.03314*, 2024.
- Tian, K., Mitchell, E., Zhou, A., Sharma, A., Rafailov, R., Yao, H., Finn, C., and Manning, C. D. Just ask for calibration: Strategies for eliciting calibrated confidence scores from language models fine-tuned with human feedback. *arXiv preprint arXiv:2305.14975*, 2023.
- Vaswani, A., Shazeer, N., Parmar, N., Uszkoreit, J., Jones, L., Gomez, A. N., Kaiser, Ł., and Polosukhin, I. Attention is all you need. *Advances in neural information processing systems*, 30, 2017.
- Wang, X., Wei, J., Schuurmans, D., Le, Q., Chi, E., Narang, S., Chowdhery, A., and Zhou, D. Self-consistency improves chain of thought reasoning in language models. *arXiv preprint arXiv:2203.11171*, 2022.
- Wei, J., Wang, X., Schuurmans, D., Bosma, M., Xia, F., Chi, E., Le, Q. V., Zhou, D., et al. Chain-of-thought prompting elicits reasoning in large language models. *Advances in neural information processing systems*, 35: 24824–24837, 2022.
- Xiong, M., Hu, Z., Lu, X., Li, Y., Fu, J., He, J., and Hooi, B. Can llms express their uncertainty? an empirical evaluation of confidence elicitation in llms. *arXiv preprint arXiv:2306.13063*, 2023.
- Xue, M., Liu, D., Lei, W., Ren, X., Yang, B., Xie, J., Zhang, Y., Peng, D., and Lv, J. Dynamic voting for efficient reasoning in large language models. In *Findings of the Association for Computational Linguistics: EMNLP 2023*, pp. 3085–3104, 2023.
- Yang, C., Si, Q., Duan, Y., Zhu, Z., Zhu, C., Li, Q., Lin, Z., Cao, L., and Wang, W. Dynamic early exit in reasoning models. *arXiv preprint arXiv:2504.15895*, 2025.
- Zhang, A., Chen, Y., Pan, J., Zhao, C., Panda, A., Li, J., and He, H. Reasoning models know when they’re right: Probing hidden states for self-verification. *arXiv preprint arXiv:2504.05419*, 2025a. URL <https://arxiv.org/abs/2504.05419>.
- Zhang, L., Hosseini, A., Bansal, H., Kazemi, M., Kumar, A., and Agarwal, R. Generative verifiers: Reward modeling as next-token prediction, 2024. URL <https://arxiv.org/abs/2408.15240>, 1, 2024.
- Zhang, Z., Zheng, C., Wu, Y., Zhang, B., Lin, R., Yu, B., Liu, D., Zhou, J., and Lin, J. The lessons of developing process reward models in mathematical reasoning. *arXiv preprint arXiv:2501.07301*, 2025b.

A. Experimental Details

A.1. Details on Baseline methods

A.1.1. SINGLE-SEQUENCE BASELINES

To show that the interaction between sequences does really benefit the classification performance of MSV, we compare MSV trained on $N > 1$ against MSV trained on $N = 1$, which serves as a controlled baseline. We abbreviate MSV trained on N sequences simply as MSV_N . As another baseline, we follow [Zhang et al. \(2025a\)](#) and train a 2-layer MLP ‘‘Probe’’ on the last token representations $h_{k, L_k}^{(n)}$ to predict the correctness of answers $a_k^{(n)}$. We find that the Probe serves as a strong baseline that often matches or even exceeds the performance of MSV_1 .

We focus on white-box methods in our paper, and do not consider generative verifiers ([Zhang et al., 2024](#)) or multi-agent debate ([Du et al., 2023](#)). This is because their training and inference costs lie on a different order of magnitude compared to the white-box methods that only require one forward pass. Their training scheme is also very different, often involving reinforcement learning. Altogether these factors make such methods inappropriate to compare against MSV which operates on the hidden states of LLMs with a single forward pass per prediction.

There are also training-free methods for calibration, such as using the base LLM’s token probabilities on the answer tokens ([Yang et al., 2025](#)). Specifically, we use the geometric mean of probabilities over all tokens in an answer, to estimate the answer’s correctness.

$$s_k^{(n)} = \left(\prod_{i=1}^{L_k^{(n)}} p_{\text{LLM}} \left(a_{k,i}^{(n)} \mid \text{tokens}_{<a_{k,i}^{(n)}} \right) \right)^{1/L_k^{(n)}}.$$

A.1.2. AGGREGATION BASELINES

We can further complement the single-sequence baselines with aggregation methods that combine predictions across multiple sequences through simple heuristics. Although prior work has not investigated explicit aggregation of single-sequence baselines for improving the classification of individual candidates, we introduce a baseline, *Weighted Voting* (WV), inspired by the weighted best-of-N approach ([Li et al., 2022](#)), as follows: for each equivalence class of symbolically identical answers, we aggregate its answers’ correctness probabilities by summing them, and normalize the probabilities across equivalence classes. Performing best-of-N with the WV probabilities is equivalent to weighted best-of-N, which picks the equivalence class with the biggest aggregate probability. In the streaming setting, we can also perform weighted voting for candidate $a_k^{(n)}$ by aggregating and normalizing over the symbolically equivalent ones that come before time $\tau_k^{(n)}$. However, when done naively, this can disrupt the predictions at the early token positions, due to a lack of other existing candidates. For instance, weighted voting will always assign a probability of one to the first output candidate, since there are not other candidates to normalize over. Therefore, we set a threshold $R \in \mathbb{Z}$ such that weighted voting is performed only when the number of candidates exceeds R at time $\tau_k^{(n)}$. We find that $R = 16$ yields good overall performance and use this setting throughout our experiments with WV in the **Streaming Answers** setting.

We also propose a training-free baseline inspired by *Self-Consistency* ([Wang et al., 2022](#)) that only uses the vote count (number of symbolically identical answers) to score each answer. Specifically, we score each answer $a_k^{(n)}$ with

$$s_k^{(n)} = \sum_{m=1}^N \mathbf{1}[a_1^{(n)} \sim a_1^{(m)}] / N$$

for Terminal Answers. For the **Streaming Answers** setting, we similarly use the fraction of symbolically identical answers among all that have been decoded until time $\tau_k^{(n)}$, again using the threshold $R = 16$ to prevent miscalibration at the early candidates. Note that the self-consistency baseline is equivalent to the weighted voting baseline with a verifier that outputs a constant score.

A.2. Details on Datasets and Models

The pre-trained model and datasets used in our experiments are summarized below.

Models.

- **DeepSeek-R1-Distill-Qwen-1.5B**: <https://huggingface.co/deepseek-ai/DeepSeek-R1-Distill-Qwen-1.5B>, licensed under MIT License.¹

Datasets.

- **MATH-500**: <https://huggingface.co/datasets/HuggingFaceH4/MATH-500>, licensed under MIT License.²
- **Olympiad Bench**: <https://huggingface.co/datasets/Hothon/OlympiadBench>, licensed under MIT License.³
- **AMC12**: https://huggingface.co/datasets/rulins/amc12_22-24, not openly licensed; usage is subject to MAA AMC policies.⁴
- **AIME**: <https://www.kaggle.com/datasets/hemishveeraboina/aime-problem-set-1983-2024>, licensed under CC0 License.⁵
- **Omni-MATH**: <https://huggingface.co/datasets/KbsdJames/Omni-MATH>, dataset files licensed under Apache-2.0 License.⁶
- **DeepMath-103K**: <https://huggingface.co/datasets/zwhe99/DeepMath-103K>, licensed under MIT License.⁷

We use the DeepSeek-R1-Distill-Qwen-1.5B model (Guo et al., 2025) as our base LLM that generates the reasoning traces and answers to reasoning problems. All training data for our verifier models are generated with the base LLM on problems in the DeepMath-103K dataset, which underwent careful decontamination of public reasoning evaluation datasets, including all five of our evaluation datasets (He et al., 2025). This reduces the possibility that the verifier is memorizing the training data to correctly classify solutions generated on our evaluation sets. We evaluate our model on the MATH dataset (Hendrycks et al., 2021), the AMC12 problems between 2022 and 2024, the AIME problems between 1983 and 2024, OlympiadBench (He et al., 2024), and Omni-MATH (Gao et al., 2024). We use 224 and 64 randomly chosen problems from DeepMath-103K as our training and validation sets, respectively. Each evaluation dataset is randomly subsampled to 448 problems. We generate 64 responses from the base LLM on every problem. This creates training and validation sets with 14K and 4K sequences, respectively, and evaluation datasets with at 28K sequences. We provide justification for the training set size in Section B.10.

A.3. Details on metrics

We evaluate verifier predictions on four standard probabilistic metrics. Let $\{(p_i, y_i)\}_{i=1}^m$ denote the dataset of m predicted probabilities and their corresponding binary correctness labels.

Area Under the Receiver Operating Characteristic Curve (AUROC). The Area Under the Receiver Operating Characteristic Curve (AUROC) measures the probability that a randomly chosen positive example receives a higher score than a randomly chosen negative example:

$$\text{AUROC} = \Pr [p^+ > p^-] + \frac{1}{2} \Pr [p^+ = p^-],$$

where p^+ and p^- are the predicted probabilities for a random positive and negative sequence, respectively.

Brier score. The Brier score (Brier, 1950) is the mean squared error between predicted probabilities and binary outcomes:

$$\text{Brier} = \frac{1}{m} \sum_{i=1}^m (p_i - y_i)^2.$$

Lower values indicate better calibrated and sharper probabilities.

¹<https://huggingface.co/deepseek-ai/DeepSeek-R1-Distill-Qwen-1.5B/blob/main/LICENSE>

²<https://github.com/openai/prm800k/blob/main/LICENSE>

³<https://github.com/OpenBMB/OlympiadBench/blob/main/LICENSE>

⁴<https://maa.org/student-programs/amc/maa-american-mathematics-competitions-policies/>

⁵<https://www.kaggle.com/datasets/hemishveeraboina/aime-problem-set-1983-2024>

⁶<https://huggingface.co/datasets/KbsdJames/Omni-MATH>

⁷<https://github.com/zwhe99/DeepMath/blob/main/LICENSE>

Negative Log-Likelihood (NLL). The negative log-likelihood, or log loss, evaluates the quality of probabilistic predictions:

$$\text{NLL} = -\frac{1}{m} \sum_{i=1}^m \left(y_i \log p_i + (1 - y_i) \log(1 - p_i) \right).$$

Expected Calibration Error (ECE). The Expected Calibration Error (Naeini et al., 2015; Guo et al., 2017) measures the discrepancy between a model’s predicted confidences and the actual accuracies. To compute ECE, predictions are grouped into J bins based on their confidence scores. The ECE is the weighted average of the absolute difference between the mean confidence and the mean accuracy within each bin:

$$\text{ECE} = \sum_{j=1}^J \frac{|B_j|}{m} |\text{acc}(B_j) - \text{conf}(B_j)|,$$

where B_j is the set of indices of predictions whose confidence p_i falls into the j -th bin, $\text{acc}(B_j) = \frac{1}{|B_j|} \sum_{i \in B_j} y_i$ is the accuracy of that bin, and $\text{conf}(B_j) = \frac{1}{|B_j|} \sum_{i \in B_j} p_i$ is the average confidence of that bin. We use $J = 10$ in all our reports of ECE.

Best-of-N Accuracy. Best-of-N Accuracy is the primary metric for evaluating the effectiveness of the verifier-guided selection process in the Terminal Answers setting. For each problem, the system generates N candidate answers. A verifier then provides a score for each candidate, and the one with the highest score p^\dagger , denoted a^\dagger , is selected as the final output. The accuracy is the fraction of problems in an evaluation set Q for which this selected answer is equivalent to the ground truth answer a^* . Formally, it is expressed as:

$$\text{Accuracy} = \frac{1}{|Q|} \sum_{q \in Q} y_q^\dagger, \text{ where } y_q^\dagger = \mathbf{1}[a_q^\dagger \sim a_q^*]$$

and a_q^\dagger is the verifier-selected answer for problem q , and a_q^* is the ground truth. A higher accuracy indicates a more effective verifier that is better at identifying the correct solution from the pool of candidates, thus serving as a direct measure of downstream task performance.

Best-of-N ECE and Brier score. Best-of-N ECE and Brier scores are the ECE and Brier scores computed over the set $\{(p_q^\dagger, y_q^\dagger)\}$ best-of-N confidence and correctness pairs.

Area Under the Tradeoff Curve. Sliding the threshold λ between 0 and 1 shifts the point on the accuracy-latency tradeoff curve. One can readily show that latency increases monotonically with increasing threshold λ , due to more conservative early stopping. Moreover, the latency at $\lambda = 0$ and $\lambda = 1$ are constant with fixed dataset and N . It is thus appropriate to quantify the aptness of a verifier at early stopping with a single scalar value, namely the area under the tradeoff curve (AUTC). Importantly, a verifier that achieves higher accuracy than another verifier at every latency will also be characterized by a higher value of AUTC. This is also logically equivalent to requiring lower latency to achieve the same target accuracy.

A.4. Details on Experiments

We adopt the setup and terminology of Terminal/Streaming answers from Section 3, and follow the experimental protocol of Section 4.1. Below we provide additional details necessary for reproducibility.

Optimizer and schedule. All models are trained with AdamW, combined with the Hugging Face default constant-with-warmup scheduler (default warmup ratio). Gradient clipping is applied with `max_grad_norm` set to 1.0.

Learning rate selection. We sweep learning rates in $\{1e-5, 5e-5, 1e-4, 5e-4, 1e-3, 5e-3\}$ and choose the best value by cross-validation on the validation split.

Final learning rates. The probe MLP is trained with $\text{lr} = 1e-3$. All other modules use $\text{lr} = 5e-5$, except the MMTB mixture weights w ($\text{lr} = 1e-1$) and the per-sequence embeddings $e^{(n)}$ ($\text{lr} = 1e-3$).

Category	Setting (ours)
Optimizer	AdamW
LR schedule	constant-with-warmup (HF defaults)
LR sweep	{ $1e-5$, $5e-5$, $1e-4$, $5e-4$, $1e-3$, $5e-3$ } (CV on validation)
Final LRs	Probe: $1e-3$; Others: $5e-5$; w : $1e-1$; $e^{(n)}$: $1e-3$
Probe arch.	2-layer MLP, hidden size 1024
MSV depth	1 Multi-Mask Transformer Block
Batch	64
Gradient accumulation steps	1
Epochs	Terminal: 1; Streaming: 2 (4 only during LR sweep)
Gradient clipping	max_grad_norm = 1.0
Gradient checkpointing	Not used
Max sequence length	4096
Temperature	1.0
Answer length	≤ 40 tokens (after elicitation)

Table 3. Summary of implementation and hyperparameters.

Table 4. Token counts required to achieve the target accuracy on MATH.

N	Probe	MSV_N
4	3699.5	2886.3
16	4022.8	1616.4
64	4131.8	1407.4

Model capacity. The MSV verifier consists of a single Multi-Mask Transformer Block (one transformer layer) whose width and attention heads follow the base model. The probe is implemented as a 2-layer MLP with hidden size 1024.

Batching and epochs. We use a global batch size of 64 with no gradient accumulation. Training runs for 1 epoch on Terminal data and 2 epochs on Streaming data. For LR selection, up to 4 epochs are used on the validation split.

Decoding and prompting. We follow the elicitation protocol in the main paper, using the boxed `Final Answer` format and the “wait” delimiter for Streaming. Decoding uses temperature = 1.0 without further heuristics. Each output is allowed up to 4096 tokens, with the elicited final answer truncated to 40 tokens.

Hardware. All experiments fit within a single RTX A6000 GPU (48 GB memory) per model.

B. Additional Experiments

B.1. Latency Analysis in the Streaming Answers Setting

To substantiate our claim that MSV improves the accuracy-latency tradeoff compared to baselines, we provide detailed measurements of latency on the MATH dataset in the Streaming Answers setting. For each verifier and N , we measure the minimum latency at which the respective accuracy matches or surpasses the highest accuracy achievable by Probe (the target accuracy). We break down the latency into three components: chain-of-thought generation, intermediate answer generation, and verifier inference.

Token Efficiency. Table 4 reports the token positions at which each verifier reaches the target accuracy for different values of N . MSV_N consistently achieves the same accuracy as Probe using substantially fewer tokens across all values of N , with the gap widening as N increases.

Wall-Clock Time Analysis. We measure the actual wall-clock time for each of the three components using batched computation on a single A6000 GPU. Tables 5, 6, and 7 report the average latency for chain-of-thought generation, intermediate answer generation, and verifier inference, respectively. While MSV incurs additional overhead for verifier inference due to processing multiple sequences, this overhead remains small in absolute terms (under 4 seconds even for $N = 64$) and is more than compensated by the substantial reductions in generation time. Note that there is also latency incurred by running the symbolic equivalence checker SymPy, which was on average 0.34 seconds, but omit from our calculation.

Table 5. Average latency(\downarrow) of CoT generation on MATH (seconds).

N	Probe	MSV $_N$
4	87.5	68.3
16	175.4	70.4
64	568.7	193.7

 Table 6. Average latency(\downarrow) of intermediate answer generation on MATH (seconds).

N	Probe	MSV $_N$
4	0.9	0.7
16	1.9	0.7
64	6.2	2.1

End-to-End Latency. Table 8 reports the total end-to-end latency by summing the three components. MSV $_N$ achieves lower latency than Probe across all values of N , with reductions ranging from 21.8% to 65.4%. These results confirm that MSV not only improves token efficiency but also delivers practical wall-clock time improvements in the Streaming Answers setting.

Training latency. In the Terminal Answers setting, training takes around 50 minutes regardless of the verifier. In the Streaming Answers setting, training of Probe, MSV 1, MSV 4, MSV 16, and MSV 64 takes around 105, 105, 105, 110, and 145 minutes, respectively. We performed cross-validation on the number of epochs, meaning that running more epochs on Probe, MSV 1, or MSV 4 doesn’t improve their performance.

B.2. Discussion on Parallel Early Stopping

Although usually not the case in practice, one can increase the value of N without increasing the latency of a single decoding step, e.g. by scaling the number of GPUs proportionally with N . In this hypothetical setting, one can “buy” more N to both improve task performance *and* reduce latency compared to single-sequence decoding! Figure 8 shows that latency of best-of- N generally increases with the number of sequences N , because the maximum sequence length strictly increases in expectation with increasing N :

$$\mathbb{E}[L^{(1)}] < \mathbb{E}[\max(L^{(1)}, \dots, L^{(4)})] < \mathbb{E}[\max(L^{(1)}, \dots, L^{(16)})] < \dots$$

where $L^{(i)}$ is the length of the fully decoded i th sequence. On the other hand, the figure shows that parallel early stopping with MSV $_N$ allows for reduction of latency *and* improved task performance, with increasing N . We would like to note that this claim only holds true in the hypothetical setting where latency per token position is constant regardless of N , and where the overhead incurred by the forward pass of MSV $_N$ is minimal. We don’t claim that any of these two are true in our experimental setup. Instead, we point at the potential of our novel framework, that contrasts starkly with previous multi-sequence early stopping frameworks which introduce latency that grows about linearly with N —and thus wouldn’t have even fit in our plots.

B.3. Ablation Study of Attention Masks

To assess the contribution of each attention mask in MSV, we conduct an ablation study by removing each mask individually and evaluating the resulting model’s calibration performance. Table 9 reports the Brier score, AUROC, and negative log-likelihood (NLL) of the Streaming MSV $_{16}$ model on AIME, with each mask ablated in turn.

The results show that all masks contribute to the overall performance, but the equivalence and within-sequence masks are especially important. Removing the equivalence mask increases the Brier score by 18.4% and substantially degrades AUROC and NLL, indicating that cross-sequence attention to equivalent answers is critical for effective verification. Removing the within-sequence mask also leads to noticeable degradation across all metrics. In contrast, removing the full mask has the smallest effect, suggesting that the more specialized masks capture the most relevant information for verification.

Table 7. Average latency of verifier inference on MATH (seconds).

N	Probe	MSV_N
4	0.0003	0.1
16	0.001	0.4
64	0.005	3.1

Table 8. Average end-to-end latency on MATH (seconds).

N	Probe	MSV_N	Reduction
4	88.5	69.2	21.8%
16	177.3	71.6	59.6%
64	575.0	199.0	65.4%

Motivation for Multiple Masks. Our decision to use multiple specialized masks was informed by preliminary experiments in which we allowed the verifier to attend to all tokens in the sequence, including chain-of-thought tokens. We initially hypothesized that, since attending to more tokens strictly increases the available information, specialized masks would be unnecessary.

Contrary to this expectation, we observed that restricting attention to only the answer tokens led to substantially better generalization. This indicated that transformers can be distracted by less critical information, and that explicitly guiding attention toward the most informative parts of the sequence improves performance. Building on this insight, we tested more specialized masks that attend only to semantically related subsets of answers (e.g., equivalent answers within and across sequences). The ablation results confirm that appropriately combining these specialized masks yields the strongest overall performance, as each mask captures complementary aspects of the multi-sequence structure.

B.4. Ablation: Logit Averaging in Streaming Answers

In Section 3.2, we presented several design choices of MSV without extensive justification. The most notable is the absence of logit averaging in the prediction stage of the Streaming Answers setting. We therefore design a version of MSV that uses logit averaging during training and inference. Since the predictions have to respect causality in the Streaming Answers setting, we average the logits over all symbolically equivalent answers that come before in time. We train the ablated model architecture with $N = 16$, and evaluate on the AIME dataset. We report the standard calibrations metrics in Table 10. One can see that logit averaging actually hurts the performance of MSV_{16} , potentially due to the low quality logits in the early parts of the sequences that become aggregated even in later parts of the sequences through averaging.

B.5. MSV with Different Base Language Models

In addition to the main experiments, we evaluate the robustness of MSV across different base language models and datasets. Concretely, we consider three additional base LMs: DeepSeek-R1-Distill-Llama-8B, Qwen3-1.7B in thinking mode, and Llama-3.2-1B-Instruct. Unless otherwise stated, we reuse the same training setup and hyperparameters as in the main experiments.

DeepSeek-R1-Distill-Llama-8B on AIME. We first consider a larger base model, DeepSeek-R1-Distill-Llama-8B, in the AIME Terminal Answers setup. Table 11 reports calibration metrics for different verifiers, and Table 12 reports best-of-64 accuracy. Increasing N consistently improves the calibration of MSV, and MSV_{64} yields the highest AUROC and lowest Brier score. When used for best-of-64 selection, MSV_{64} also outperforms all baselines, including Probe with and without weighted voting.

Qwen3-1.7B (thinking mode) on AIME. We next evaluate Qwen3-1.7B in thinking mode on AIME. As shown in Table 13, MSV achieves progressively better calibration as N increases, with substantial gains in both Brier score and AUROC compared to Probe. Table 14 shows that MSV_{64} also improves best-of-64 accuracy over all baselines.

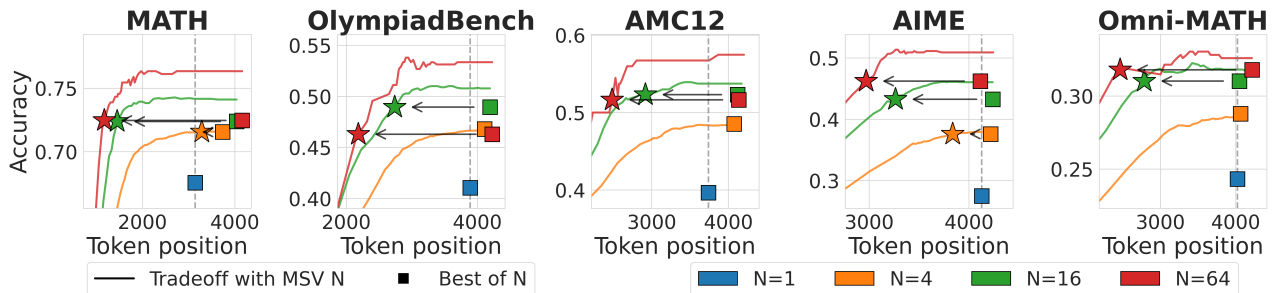


Figure 8. Accuracy-latency tradeoff curves of parallel early stopping with MSV_N , with multiple values of N overlapped in a single plot. Square markers represent best-of- N with the verifier MSV_1 trained only on terminal answers. Star markers are assigned to points on tradeoff curves that achieve the same accuracy as best-of- N .

Table 9. Mask ablation results on AIME with MSV_{16} in the Streaming Answers setting.

Metric	MSV_{16}	w/o full	w/o equiv.	w/o within-seq	w/o within-ans
Brier ↓	0.038	0.040	0.045	0.048	0.050
AUROC ↑	0.953	0.953	0.922	0.945	0.949
NLL ↓	0.150	0.157	0.236	0.192	0.169

Llama-3.2-1B-Instruct on MATH. Finally, we consider Llama-3.2-1B-Instruct, a non-reasoning model whose accuracy on AIME is close to zero. For this model we therefore train and evaluate on the MATH train/test splits. Table 15 reports calibration metrics, and Table 16 reports best-of-64 accuracy. Even in this lower-accuracy regime, MSV_{16} and MSV_{64} significantly improve calibration over Probe, and MSV_{64} achieves the best best-of-64 accuracy.

Overall, these results indicate that the benefits of MSV are not restricted to a particular base model or dataset: across all three additional base LMs, increasing N systematically improves both calibration and best-of- N accuracy.

B.6. Computational Complexity of MSV

In the Streaming Answers setting, N sequences are decoded in parallel. Assuming delimiters are uniformly distributed throughout a sequence, the total number of delimiters across all sequences—and thus the total number of forward passes through MSV—is $O(NL)$, where L is the average sequence length. The computational cost of each MSV forward pass is linear in the number of answer tokens it attends to, which is also $O(NL)$. Crucially, the cost is not quadratic because we only need to query the attention mechanism with the last token of the most recent answer, i.e. we use KV caching. This yields a total MSV computational cost of $O(N^2L^2)$, whereas the decoding of the N sequences itself scales as $O(NL^2)$. Thus, MSV adds an extra factor in N , while the dependence on sequence length L matches that of the underlying decoding process. This is a common issue among methods that incorporate information between sequences, but is usually shown not to be a significant bottleneck for practical values of N (Du et al., 2023; Rodionov et al., 2025). We provide a simple yet effective solution in Section B.7.

B.7. Scaling with MSV M for Large N

To address scalability concerns when N is large (e.g., in the order of hundreds), we employ a simple and effective remedy: use MSV_M with N parallel sequences, where M is kept constant as we scale N . This is achieved by partitioning the N sequences into N/M groups, each of size M , and processing each group through MSV_M independently. This reduces the computational complexity from $O(N^2L^2)$ to $O(MNL^2)$, or equivalently $O(NL^2)$ when treating M as a constant.

Table 17 reports the area under the tradeoff curve (AUTC) in the $N = 128$ setting on the AIME dataset using this partitioning scheme. We observe that MSV_M provides a better tradeoff than Probe’s vanilla verification, even when $M \neq N$. Importantly, because M is fixed and small, MSV’s additional overhead remains at most proportional to the cost of decoding the sequences themselves, while still benefiting from joint reasoning within each group of size M . This makes it practical to scale N beyond 64–128, without incurring a superlinear blow-up in cost relative to standard parallel decoding with vanilla verification.

Table 10. Ablation of MSV architectural choices in the Streaming Answers setting. We report calibration metrics on the AIME dataset.

Method	AUROC \uparrow	Brier \downarrow	NLL \downarrow
MSV ₁	0.906 \pm 0.008	0.064 \pm 0.003	0.241 \pm 0.011
MSV ₁₆	0.953 \pm 0.007	0.038 \pm 0.003	0.150 \pm 0.011
Ablation	0.936 \pm 0.0016	0.047 \pm 0.009	0.190 \pm 0.0333

Table 11. Brier score and AUROC of verifiers with DeepSeek-R1-Distill-Llama-8B on AIME.

	Probe	MSV ₁	MSV ₁₆	MSV ₆₄
Brier \downarrow	0.0668	0.0770	0.0298	0.0283
AUROC \uparrow	0.9668	0.9746	0.9908	0.9923

B.8. Sensitivity to Delimiter Choice in Streaming Answers

In the Streaming Answers setting, we use delimiter tokens to segment sequences into intermediate answers. While our main experiments use “Wait” as the delimiter, we investigate the sensitivity of MSV to this choice by evaluating two alternative delimiters: “Alternatively” and “But”, both of which frequently appear as the first token of a paragraph in mathematical reasoning. On the AIME dataset, “Wait”, “Alternatively,” and “But” occur roughly once every 200, 900 and 400 tokens, respectively

Table 18 reports the area under the tradeoff curve (AUTC) for each delimiter-verifier combination. The results show that while the choice of delimiter does affect the absolute performance of the tradeoff, the relative ordering between verifiers remains consistent across all delimiters: MSV₁₆ consistently outperforms both Probe and MSV₁, demonstrating the robustness of our approach to delimiter selection.

B.9. Comparison with External Verifiers.

To contextualize MSV’s performance relative to commonly used verification methods in the literature, we compare against Qwen2.5-Math-PRM-7B (Zhang et al., 2025b), one of the most performant open-source verifiers. (Liu et al., 2025) We evaluate in the best-of-64 setting, where we rank all 64 terminal answers using either the external verifier or MSV₆₄. Additionally, we report results for Qwen2.5-Math-PRM-7B combined with weighted voting (WV).

Table 19 shows that MSV₆₄ consistently outperforms the external PRM across all benchmarks, with particularly substantial gains on harder datasets such as OlympiadBench, AIME, and Omni-MATH. These results demonstrate that MSV’s joint reasoning over multiple candidate solutions provides advantages beyond what can be achieved with standalone process reward models, even when those models are trained on large-scale verification datasets.

B.10. Training Set Size

Our training set consists of 224 problems sampled from the DeepMath-103K training set. While some readers may be concerned of how small this is, we sample 64 model responses per problem, yielding $224 \times 64 = 14,336$ sequences in total. This is actually about equal or larger than the datasets used in most research on probes, such as Zhang et al. (2025a) who use 1,000 sequences to show that probes can generalize to a remarkable degree with small data.

To further validate the choice of our training set size, we conducted preliminary experiments with Probe in the **Terminal Answers** setting, varying the number of training problems. Table 20 shows that performance plateaus beyond 224 problems, with doubling to 448 problems yielding no improvement. This saturation suggests that our verifiers efficiently learn the verification task with relatively few problems, which represents a practical advantage: MSV can be trained quickly without requiring extensive problem collections or prolonged training procedures.

B.11. Latency Scaling with Parallel Sequences

In Section 1, we claim that MSV *theoretically* enables parallel early stopping where latency does not grow with the number of sequences N . This claim holds in the idealized setting where computational resources (specifically, the number of GPUs) scale proportionally with N , such that the per-token decoding latency remains constant.

Table 12. Best-of-64 accuracy with DeepSeek-R1-Distill-Llama-8B on AIME.

	Probe	Probe + WV	MSV ₁	MSV ₁ + WV	MSV ₆₄
Best-of-64	0.6104	0.6337	0.6052	0.6386	0.6625

Table 13. Brier score and AUROC of verifiers with Qwen3-1.7B (thinking mode) on AIME.

	Probe	MSV ₁	MSV ₄	MSV ₁₆	MSV ₆₄
Brier ↓	0.0849	0.0770	0.0595	0.0440	0.0317
AUROC ↑	0.9530	0.9570	0.9696	0.9825	0.9878

Table 21 reports the end-to-end latency in this idealized setting when using Probe on the MATH dataset. For each value of N , we set the threshold λ such that the accuracy matches or surpasses the pass@1 baseline. The results show that the latency required to achieve this fixed target accuracy decreases with increasing N , validating our claim. However, we observe that latency saturates around $N = 64$, which is consistent with the saturation of best-of- N performance at large N (Snell et al., 2024).

B.12. MSV with Mean Across Answer Tokens

In our main experiments, MSV uses only transformer block output at the last token position of each answer in order to obtain the logit. This design choice was inherited from prior work on probes (Zhang et al., 2025a), which operate exclusively on the final hidden state. We hypothesized that the attention layer would be sufficiently expressive to aggregate relevant information from all answer tokens.

However, an alternative design is to use the mean of hidden states across all answer tokens instead of only the last token. To evaluate this variant, we compare MSV _{N} against MSV _{N} (Mean) in the Terminal Answers setting on the AIME dataset.

Table 22 shows that the mean variant provides a modest but consistent improvement in Brier score across all values of N . However, this improvement comes at a computational cost: the mean variant requires querying the attention mechanism with all answer tokens rather than just the last token, resulting in slightly higher computational overhead. Given this tradeoff and the already strong performance of the last-token variant, we use the last-token approach in our main experiments for computational efficiency.

C. Details on Method

C.1. Multi-Sequence Verifier Pseudocode

In Algorithm 1, we present a pseudocode of MSV’s forward pass.

D. Full Report of Main Experiments

This section presents the full results on our main experiments, including all benchmarks, evaluation metrics, and baselines including the training-free methods. All tables and figures are provided here in complete form for reference.

D.1. Full report on the Terminal Answers setting with trained verifiers.

Table 23 and Table 24 report all the standard calibration metrics—AUROC, BS, ECE, and NLL—in the **Terminal Answers** setting. We find that the metrics improve across all values of N across all datasets, following the trend reported in Section 4.2. Similarly, Table 25 reports the full best-of- N accuracy across all values of N . We find that the best single-sequence baselines perform almost the same but slightly better than MSV₄ at $N = 4$, and that MSV _{N} greatly improves the accuracy over the single-sequence baselines at $N = 16$ and 64. This is also consistent with our reports in Section 4.2. Finally, we show all the calibration metrics of best-of- N confidence, namely ECE and BS, in Table 26. In terms of best-of- N calibration, MSV _{N} outperform best single-sequence baselines across all values of N , implying much more reliable confidence levels.

Parallel Test-Time Scaling with Multi-Sequence Verifiers

Table 14. Best-of-64 accuracy with Qwen3-1.7B (thinking mode) on AIME.

	Probe	Probe + WV	MSV₁	MSV₁ + WV	MSV₆₄
Best-of-64	0.5223	0.5089	0.4910	0.5294	0.5491

Table 15. Brier score and AUROC of verifiers with Llama-3.2-1B-Instruct on MATH.

	Probe	MSV₁	MSV₁₆	MSV₆₄
Brier ↓	0.1236	0.1192	0.0596	0.0510
AUROC ↑	0.7856	0.7654	0.9222	0.9513

D.2. Full report on the Streaming Answers setting with trained verifiers.

Next, we analyze the full results for the **Streaming Answers** setting. Table 27 and Table 28 show the standard calibration metrics, while Table 29 reports the Area Under the Tradeoff Curve (AUTC) for parallel early stopping. Consistent with the findings in Section 4.3, the results demonstrate that MSV_N consistently and significantly outperforms all single-sequence baselines across every metric and dataset. The performance improvement scales with N , although MSV_{64} slightly deteriorates compared to MSV_{16} . The superior per-answer calibration of MSV_N directly translates to more effective early stopping, as shown by the higher AUTC scores in Table 29. The AUTC for MSV_N is substantially higher than for the baselines, quantitatively confirming that our method achieves a better accuracy-latency tradeoff.

D.3. Full report on the training-free baselines

Finally, we report the performance of the **training-free baselines** for completeness (Table 30 through Table 36). While methods like Self-Consistency and those based on token probabilities provide useful reference points, they are substantially outperformed by the trained verifiers across all settings. In the Terminal Answers setting, the trained baselines like Probe and MSV_1 are far better calibrated (Table 30 and Table 31 vs. Table 23 and Table 24). This performance gap is even more pronounced in the downstream best-of- N application, where MSV_N achieves much higher accuracy (Table 32 vs. Table 25) and produces significantly more reliable confidence scores for its chosen answers (Table 33 vs. Table 26). The training-free methods are particularly ill-suited for the Streaming Answers setting, where their poor calibration leads to very low AUTC scores (Table 36 vs. Table 29). This comprehensive comparison underscores the necessity of training a dedicated verifier to effectively leverage parallel scaling.

Parallel Test-Time Scaling with Multi-Sequence Verifiers

Table 16. Best-of-64 accuracy with Llama-3.2-1B-Instruct on MATH.

	Probe	Probe + WV	MSV₁	MSV₁ + WV	MSV₆₄
Best-of-64	0.2393	0.3402	0.1732	0.3402	0.3778

Table 17. Area Under the Tradeoff Curve on the AIME dataset with $N = 128$ parallel sequences

Method	Probe	MSV₁	MSV₄	MSV₁₆	MSV₆₄
AUTC	984.3	963.8	1060.0	1130.6	1168.9

Table 18. Area Under the Tradeoff Curve with different delimiters on the AIME dataset with $N = 16$ parallel sequences

Delimiter	Probe	MSV₁	MSV₁₆
Wait	1024.2	954.8	1078.3
Alternatively	985.9	980.0	1012.4
But	1039.3	1023.6	1070.7

Table 19. Best-of-64 performance comparison between Qwen2.5-Math-PRM-7B and MSV₆₄ across multiple mathematical reasoning benchmarks

Dataset	PRM-7B	PRM-7B + WV	MSV₆₄
MATH	0.7411	0.7433	0.7607
OlympiadBench	0.3906	0.4018	0.5366
AMC12	0.5224	0.5000	0.5866
AIME	0.4397	0.4174	0.5098
Omni-MATH	0.2344	0.2366	0.3540

Table 20. Brier score of Probe on the AIME dataset as a function of training set size

# of problems	Brier score
56	0.0833
112	0.0821
224	0.0809
448	0.0812

Table 21. End-to-end latency (in seconds) of early stopping required to achieve a fixed target accuracy (matching or surpassing pass@1) on the MATH dataset with Probe as the verifier, assuming the number of GPUs scales proportionally with N

N	Latency
1	51.8
4	25.8
16	22.9
64	17.6
128	19.6

Table 22. Brier score comparison between MSV _{N} using the last token versus the mean of answer tokens on the AIME dataset in the Terminal Answers setting.

Method	$N = 1$	$N = 4$	$N = 16$	$N = 64$
MSV _{N}	0.0819	0.0687	0.0572	0.0387
MSV _{N} (Mean)	0.0756	0.0641	0.0544	0.0382

Algorithm 1 Multi-Sequence Verifier (MSV) Forward Pass

Require: N sequences with hidden states $\{h_{k,i}^{(n)}\}$, readout time t
Ensure: Correctness predictions $\{\tilde{y}_k^{(n)}\}$ for all answers up to time t
Trainable parameters: Sequence embeddings $\{e^{(n)}\}$, QKV projections (W_Q, W_K, W_V) , mask weights $\{w_h\}$, MLP & LN, feature MLP, prediction head (\mathbf{w}, b)

- 1: $U^{(t)} \leftarrow \text{concat} \left(\left\{ \left\{ \{h_{k,i}^{(n)} + e^{(n)}\}_{i=1}^{L_k^{(n)}} \right\}_{\tau_k^{(n)} \leq t} \right\}_{n=1}^N \right)$
- 2: Compute query, key, value projections: $(Q_h^{(t)}, K_h^{(t)}, V_h^{(t)})_{h=1}^H$
- 3: **for** each head $h = 1, \dots, H$ and mask $j = 1, \dots, J$ **do**
- 4: $A_{h,j}^{(t)} \leftarrow \text{softmax} \left(\frac{Q_h^{(t)} (K_h^{(t)})^\top}{\sqrt{d}} + \log M_j \right) V_h^{(t)}$
- 5: **end for**
- 6: $\tilde{U}^{(t)} \leftarrow \sum_{h=1}^H \sum_{j=1}^J \alpha_{h,j} A_{h,j}^{(t)}$ where $(\alpha_{h,1}, \dots, \alpha_{h,J}) = \text{softmax}(\mathbf{w}_h)$
- 7: $Z^{(t)} \leftarrow (U^{(t)} + \tilde{U}^{(t)}) + \text{MLP}(\text{LN}(U^{(t)} + \tilde{U}^{(t)}))$
- 8: **for** each answer $a_k^{(n)}$ generated by time t **do**
- 9: Compute $\gamma_k^{(n)} \leftarrow \frac{1}{N} \sum_{m=1}^N \mathbf{1}[a_k^{(m)} \sim a_k^{(n)}]$
- 10: $\tilde{z}_k^{(n)} \leftarrow z_{k,L_k^{(n)}}^{(n)} + \text{MLP}(\gamma_k^{(n)})$
- 11: **end for**
- 12: **if** Terminal Answers mode **then**
- 13: $\tilde{y}_1^{(n)} \leftarrow \sigma \left(\frac{1}{|\mathcal{C}^{(n)}|} \sum_{m \in \mathcal{C}^{(n)}} (\mathbf{w}^\top \tilde{z}_1^{(m)} + b) \right)$ for all n
- 14: **else if** Streaming Answers mode **then**
- 15: $\tilde{y}_k^{(n)} \leftarrow \sigma(\mathbf{w}^\top \tilde{z}_k^{(n)} + b)$ for all (n, k)
- 16: **end if**
- 17: **return** $\{\tilde{y}_k^{(n)}\}$

Table 23. AUROC and Brier score of verifiers trained and evaluated on terminal answers.

	MATH		OlympiadBench		AMC12		AIME		Omni-MATH	
	AUROC \uparrow	Brier \downarrow								
Probe	0.8790 \pm 0.0052	0.1346 \pm 0.0107	0.9022 \pm 0.0038	0.1271 \pm 0.0144	0.8994 \pm 0.0062	0.1438 \pm 0.0214	0.9461 \pm 0.0034	0.0859 \pm 0.0147	0.8836 \pm 0.0008	0.1340 \pm 0.0252
MSV 1	0.8566 \pm 0.0166	0.1460 \pm 0.0063	0.8926 \pm 0.0048	0.1310 \pm 0.0061	0.8890 \pm 0.0080	0.1498 \pm 0.0099	0.9469 \pm 0.0025	0.0819 \pm 0.0066	0.8711 \pm 0.0062	0.1460 \pm 0.0103
Probe + WV 4	0.7930 \pm 0.0033	0.1649 \pm 0.0008	0.8494 \pm 0.0018	0.2164 \pm 0.0017	0.8222 \pm 0.0040	0.2367 \pm 0.0010	0.8624 \pm 0.0037	0.2100 \pm 0.0017	0.8251 \pm 0.0025	0.2704 \pm 0.0028
MSV 1 + WV 4	0.7920 \pm 0.0023	0.1656 \pm 0.0005	0.8479 \pm 0.0009	0.2168 \pm 0.0013	0.8204 \pm 0.0026	0.2371 \pm 0.0014	0.8636 \pm 0.0012	0.2096 \pm 0.0008	0.8219 \pm 0.0012	0.2711 \pm 0.0021
MSV 4	0.8945 \pm 0.0135	0.1348 \pm 0.0055	0.9298 \pm 0.0036	0.1108 \pm 0.0064	0.9125 \pm 0.0127	0.1406 \pm 0.0123	0.9628 \pm 0.0040	0.0687 \pm 0.0132	0.8986 \pm 0.0025	0.1296 \pm 0.0128
Probe + WV 16	0.8228 \pm 0.0018	0.1416 \pm 0.0007	0.9028 \pm 0.0022	0.1588 \pm 0.0010	0.8728 \pm 0.0030	0.1759 \pm 0.0025	0.9092 \pm 0.0055	0.1368 \pm 0.0039	0.8714 \pm 0.0026	0.1921 \pm 0.0006
MSV 1 + WV 16	0.8228 \pm 0.0033	0.1425 \pm 0.0003	0.9008 \pm 0.0010	0.1612 \pm 0.0008	0.8691 \pm 0.0029	0.1786 \pm 0.0018	0.9057 \pm 0.0024	0.1404 \pm 0.0015	0.8672 \pm 0.0010	0.1946 \pm 0.0008
MSV 16	0.9062 \pm 0.0182	0.1255 \pm 0.0038	0.9469 \pm 0.0021	0.1005 \pm 0.0064	0.9231 \pm 0.0144	0.1315 \pm 0.0095	0.9732 \pm 0.0015	0.0572 \pm 0.0114	0.9109 \pm 0.0034	0.1258 \pm 0.0113
Probe + WV 64	0.8346 \pm 0.0030	0.1370 \pm 0.0009	0.9173 \pm 0.0026	0.1466 \pm 0.0014	0.8844 \pm 0.0050	0.1649 \pm 0.0033	0.9216 \pm 0.0066	0.1217 \pm 0.0050	0.8830 \pm 0.0029	0.1764 \pm 0.0012
MSV 1 + WV 64	0.8364 \pm 0.0019	0.1380 \pm 0.0005	0.9130 \pm 0.0014	0.1499 \pm 0.0009	0.8829 \pm 0.0034	0.1682 \pm 0.0023	0.9168 \pm 0.0031	0.1264 \pm 0.0018	0.8788 \pm 0.0012	0.1794 \pm 0.0008
MSV 64	0.9049 \pm 0.0162	0.1261 \pm 0.0036	0.9546 \pm 0.0026	0.0835 \pm 0.0074	0.9290 \pm 0.0089	0.1267 \pm 0.0039	0.9822 \pm 0.0003	0.0387 \pm 0.0066	0.9286 \pm 0.0034	0.1041 \pm 0.0085

Table 24. ECE and NLL of verifiers trained and evaluated on terminal answers.

	MATH		OlympiadBench		AMC12		AIME		Omni-MATH	
	ECE \downarrow	NLL \downarrow								
Probe	0.0726 \pm 0.0401	0.4391 \pm 0.0485	0.0700 \pm 0.0517	0.4172 \pm 0.0437	0.1064 \pm 0.0581	0.4680 \pm 0.0730	0.1024 \pm 0.0483	0.3115 \pm 0.0488	0.1206 \pm 0.0589	0.4394 \pm 0.0817
MSV 1	0.0849 \pm 0.0190	0.4787 \pm 0.0291	0.0806 \pm 0.0232	0.4363 \pm 0.0213	0.1279 \pm 0.0304	0.4913 \pm 0.0364	0.1043 \pm 0.0250	0.2993 \pm 0.0221	0.1446 \pm 0.0288	0.4881 \pm 0.0345
Probe + WV 4	0.1655 \pm 0.0005	1.1793 \pm 0.0029	0.2457 \pm 0.0007	1.2096 \pm 0.0066	0.2633 \pm 0.0008	1.4417 \pm 0.0034	0.2703 \pm 0.0009	1.1423 \pm 0.0054	0.3313 \pm 0.0003	1.4971 \pm 0.0116
MSV 1 + WV 4	0.1654 \pm 0.0004	1.1819 \pm 0.0031	0.2461 \pm 0.0003	1.2106 \pm 0.0058	0.2641 \pm 0.0004	1.4449 \pm 0.0056	0.2714 \pm 0.0006	1.1412 \pm 0.0020	0.3321 \pm 0.0003	1.4995 \pm 0.0094
MSV 4	0.1065 \pm 0.0177	0.4677 \pm 0.0362	0.0821 \pm 0.0267	0.3663 \pm 0.0206	0.1306 \pm 0.0357	0.4793 \pm 0.0424	0.0908 \pm 0.0374	0.2472 \pm 0.0384	0.1265 \pm 0.0309	0.4424 \pm 0.0423
Probe + WV 16	0.1293 \pm 0.0009	0.9282 \pm 0.0023	0.1644 \pm 0.0015	0.6382 \pm 0.0023	0.1800 \pm 0.0017	0.8120 \pm 0.0069	0.1579 \pm 0.0032	0.5808 \pm 0.0108	0.2256 \pm 0.0010	0.8281 \pm 0.0047
MSV 1 + WV 16	0.1290 \pm 0.0007	0.9299 \pm 0.0029	0.1655 \pm 0.0005	0.6443 \pm 0.0030	0.1824 \pm 0.0004	0.8198 \pm 0.0064	0.1611 \pm 0.0012	0.5922 \pm 0.0033	0.2275 \pm 0.0005	0.8366 \pm 0.0053
MSV 16	0.1127 \pm 0.0108	0.4615 \pm 0.0291	0.0869 \pm 0.0197	0.3289 \pm 0.0200	0.1317 \pm 0.0197	0.4724 \pm 0.0414	0.0844 \pm 0.0234	0.2079 \pm 0.0290	0.1268 \pm 0.0205	0.4385 \pm 0.0411
Probe + WV 64	0.1205 \pm 0.0011	0.7788 \pm 0.0038	0.1437 \pm 0.0018	0.4894 \pm 0.0039	0.1611 \pm 0.0026	0.6564 \pm 0.0086	0.1288 \pm 0.0037	0.4265 \pm 0.0148	0.1999 \pm 0.0014	0.6564 \pm 0.0032
MSV 1 + WV 64	0.1202 \pm 0.0008	0.7732 \pm 0.0032	0.1451 \pm 0.0007	0.5024 \pm 0.0022	0.1664 \pm 0.0034	0.6646 \pm 0.0065	0.1347 \pm 0.0039	0.4444 \pm 0.0042	0.2020 \pm 0.0007	0.6662 \pm 0.0044
MSV 64	0.1204 \pm 0.0109	0.5443 \pm 0.0501	0.0556 \pm 0.0135	0.2904 \pm 0.0230	0.1085 \pm 0.0122	0.4986 \pm 0.0234	0.0350 \pm 0.0166	0.1501 \pm 0.0213	0.0867 \pm 0.0106	0.3705 \pm 0.0394

Table 25. Best-of-N accuracy, with verifiers at $N = 1, 4, 16, 64$.

N	Method	MATH	OlympiadBench	AMC12	AIME	Omni-MATH
1	Probe	0.6755±0.0000	0.4105±0.0000	0.3965±0.0000	0.2748±0.0000	0.2432±0.0000
	MSV 1	0.6755±0.0000	0.4105±0.0000	0.3965±0.0000	0.2748±0.0000	0.2432±0.0000
4	Probe	0.7197±0.0006	0.4725±0.0008	0.4861 ±0.0041	0.3771±0.0012	0.2885±0.0005
	MSV 1	0.7155±0.0024	0.4681±0.0011	0.4854±0.0043	0.3758±0.0008	0.2878±0.0018
	Probe + WV 4	0.7250 ±0.0009	0.4770 ±0.0003	0.4856±0.0030	0.3847±0.0010	0.2910 ±0.0009
	MSV 1 + WV 4	0.7224±0.0011	0.4755±0.0014	0.4845±0.0030	0.3852 ±0.0008	0.2900±0.0012
	MSV 4	0.7219±0.0012	0.4747±0.0021	0.4837±0.0020	0.3811±0.0018	0.2891±0.0015
16	Probe	0.7345±0.0014	0.5039±0.0023	0.5198±0.0037	0.4470±0.0025	0.3176±0.0020
	MSV 1	0.7238±0.0031	0.4895±0.0037	0.5231±0.0035	0.4325±0.0050	0.3102±0.0023
	Probe + WV 16	0.7450±0.0028	0.5087±0.0019	0.5254±0.0072	0.4481±0.0096	0.3162±0.0037
	MSV 1 + WV 16	0.7440±0.0025	0.5104±0.0008	0.5235±0.0055	0.4460±0.0076	0.3133±0.0039
	MSV 16	0.7472 ±0.0009	0.5154 ±0.0037	0.5399 ±0.0061	0.4615 ±0.0046	0.3198 ±0.0032
64	Probe	0.7429±0.0030	0.5112±0.0062	0.5269±0.0154	0.4897±0.0098	0.3335±0.0077
	MSV 1	0.7246±0.0058	0.4629±0.0110	0.5164±0.0119	0.4621±0.0140	0.3179±0.0061
	Probe + WV 64	0.7500±0.0032	0.5223±0.0058	0.5388±0.0073	0.4790±0.0067	0.3210±0.0017
	MSV 1 + WV 64	0.7442±0.0033	0.5210±0.0030	0.5313±0.0087	0.4714±0.0052	0.3179±0.0023
	MSV 64	0.7607 ±0.0033	0.5366 ±0.0064	0.5866 ±0.0138	0.5098 ±0.0073	0.3540 ±0.0023

 Table 26. ECE and Brier score of confidence output on best-of-N answers, with verifiers at $N = 1, 4, 16, 64$.

N	Method	MATH		OlympiadBench		AMC12		AIME		Omni-MATH	
		ECE ↓	Brier ↓								
1	Probe	0.0726±0.0401	0.2693±0.0214	0.0700±0.0517	0.2543±0.0288	0.1064±0.0581	0.2876±0.0429	0.1024±0.0483	0.1717±0.0295	0.1206±0.0589	0.2681±0.0504
	MSV 1	0.0849±0.0190	0.2920±0.0126	0.0806±0.0232	0.2620±0.0122	0.1279±0.0304	0.2995±0.0198	0.1043±0.0250	0.1638±0.0132	0.1446±0.0288	0.2920±0.0206
4	Probe	0.1168±0.0448	0.3001±0.0341	0.1510±0.0689	0.3376±0.0653	0.1801±0.0639	0.3806±0.0666	0.1703±0.0579	0.2587±0.0594	0.2298±0.0777	0.3997±0.0995
	MSV 1	0.1316±0.0206	0.3316±0.0176	0.1675±0.0276	0.3624±0.0257	0.1985±0.0293	0.3927±0.0311	0.1661±0.0269	0.2459±0.0242	0.2514±0.0319	0.4372±0.0374
	Probe + WV 4	0.1797±0.0039	0.3856±0.0043	0.3066±0.0089	0.5660±0.0129	0.3050±0.0073	0.6019±0.0122	0.3204±0.0133	0.5777±0.0180	0.4396±0.0109	0.7359±0.0210
	MSV 1 + WV 4	0.1815±0.0034	0.3871±0.0036	0.3044±0.0066	0.5642±0.0105	0.3014±0.0063	0.5945±0.0065	0.3149±0.0079	0.5680±0.0066	0.4354±0.0091	0.7306±0.0156
	MSV 4	0.1133 ±0.0187	0.3010 ±0.0118	0.1031 ±0.0345	0.2864 ±0.0178	0.1477 ±0.0412	0.3477 ±0.0268	0.1019 ±0.0489	0.2040 ±0.0319	0.1695 ±0.0402	0.3410 ±0.0364
16	Probe	0.1559±0.0369	0.3397±0.0415	0.2294±0.0679	0.4428±0.0920	0.2657±0.0607	0.5024±0.0907	0.2364±0.0601	0.3776±0.0858	0.3296±0.0823	0.5635±0.1360
	MSV 1	0.1740±0.0172	0.3818±0.0229	0.2519±0.0267	0.4830±0.0365	0.2725±0.0268	0.5147±0.0381	0.2407±0.0280	0.3754±0.0442	0.3542±0.0327	0.6170±0.0501
	Probe + WV 16	0.1353±0.0017	0.3407±0.0023	0.2073±0.0070	0.4405±0.0035	0.1988±0.0046	0.4744±0.0030	0.1633±0.0035	0.4286±0.0055	0.3195±0.0064	0.5521±0.0111
	MSV 1 + WV 16	0.1356±0.0007	0.3452±0.0024	0.2049±0.0053	0.4476±0.0042	0.2002±0.0019	0.4760±0.0014	0.1659±0.0040	0.4352±0.0036	0.3201±0.0056	0.5540±0.0093
	MSV 16	0.1160 ±0.0142	0.2905 ±0.0079	0.1059 ±0.0288	0.2859 ±0.0204	0.1462 ±0.0273	0.3516 ±0.0216	0.0876 ±0.0301	0.2067 ±0.0236	0.1776 ±0.0328	0.3583 ±0.0330
64	Probe	0.1848±0.0276	0.3802±0.0400	0.3048±0.0552	0.5520±0.0995	0.3288±0.0573	0.6132±0.1003	0.3013±0.0588	0.5159±0.1006	0.4185±0.0796	0.7348±0.1555
	MSV 1	0.2128±0.0143	0.4419±0.0240	0.3555±0.0312	0.6453±0.0520	0.3520±0.0174	0.6636±0.0295	0.3162±0.0348	0.5324±0.0653	0.4504±0.0303	0.8118±0.0537
	Probe + WV 64	0.1259±0.0029	0.3305±0.0019	0.1736±0.0020	0.4102±0.0041	0.1823±0.0155	0.4611±0.0072	0.1222±0.0168	0.4165±0.0138	0.2888±0.0049	0.5115±0.0042
	MSV 1 + WV 64	0.1300±0.0016	0.3329±0.0017	0.1769±0.0059	0.4219±0.0016	0.1929±0.0086	0.4586±0.0038	0.1302±0.0100	0.4232±0.0069	0.2920±0.0033	0.5175±0.0060
	MSV 64	0.1323 ±0.0147	0.2974 ±0.0080	0.0803 ±0.0281	0.2613 ±0.0315	0.1731 ±0.0207	0.4103 ±0.0187	0.0749 ±0.0500	0.2351 ±0.0542	0.1303 ±0.0273	0.3434 ±0.0401

Parallel Test-Time Scaling with Multi-Sequence Verifiers

Table 27. AUROC and Brier score of verifiers trained and evaluated on streaming answers.

	MATH		OlympiadBench		AMC12		AIME		Omni-MATH	
	AUROC \uparrow	Brier \downarrow								
Probe	0.8690 \pm 0.0135	0.1592 \pm 0.0101	0.8317 \pm 0.0089	0.1478 \pm 0.0232	0.8621 \pm 0.0108	0.1413 \pm 0.0195	0.9114 \pm 0.0142	0.0796 \pm 0.0105	0.8229 \pm 0.0142	0.1527 \pm 0.0242
MSV 1	0.8443 \pm 0.0223	0.1601 \pm 0.0125	0.8169 \pm 0.0135	0.1425 \pm 0.0076	0.8546 \pm 0.0104	0.1343 \pm 0.0028	0.9056 \pm 0.0076	0.0642 \pm 0.0028	0.7951 \pm 0.0125	0.1381 \pm 0.0084
Probe	0.8690 \pm 0.0135	0.1592 \pm 0.0101	0.8317 \pm 0.0089	0.1478 \pm 0.0232	0.8621 \pm 0.0108	0.1413 \pm 0.0195	0.9120 \pm 0.0141	0.0796 \pm 0.0105	0.8229 \pm 0.0142	0.1527 \pm 0.0242
MSV 1	0.8443 \pm 0.0223	0.1601 \pm 0.0125	0.8169 \pm 0.0135	0.1425 \pm 0.0076	0.8546 \pm 0.0104	0.1343 \pm 0.0028	0.9056 \pm 0.0076	0.0642 \pm 0.0028	0.7951 \pm 0.0125	0.1381 \pm 0.0084
Probe + WV 4	0.8769 \pm 0.0058	0.1563 \pm 0.0079	0.8186 \pm 0.0121	0.1493 \pm 0.0183	0.8561 \pm 0.0069	0.1381 \pm 0.0149	0.8740 \pm 0.0177	0.0768 \pm 0.0069	0.8167 \pm 0.0049	0.1246 \pm 0.0197
MSV 1 + WV 4	0.8567 \pm 0.0130	0.1629 \pm 0.0074	0.8148 \pm 0.0113	0.1435 \pm 0.0071	0.8556 \pm 0.0067	0.1310 \pm 0.0074	0.9055 \pm 0.0075	0.0657 \pm 0.0028	0.7813 \pm 0.0039	0.1293 \pm 0.0082
MSV 4	0.8917\pm0.0133	0.1324\pm0.0034	0.8683\pm0.0169	0.1197\pm0.0094	0.9002\pm0.0118	0.1068\pm0.0033	0.9312\pm0.0101	0.0472\pm0.0053	0.8327\pm0.0127	0.1160\pm0.0088
Probe	0.8690 \pm 0.0135	0.1592 \pm 0.0101	0.8317 \pm 0.0089	0.1478 \pm 0.0232	0.8621 \pm 0.0108	0.1413 \pm 0.0195	0.9120 \pm 0.0141	0.0796 \pm 0.0105	0.8229 \pm 0.0142	0.1527 \pm 0.0242
MSV 1	0.8443 \pm 0.0223	0.1601 \pm 0.0125	0.8169 \pm 0.0135	0.1425 \pm 0.0076	0.8546 \pm 0.0104	0.1343 \pm 0.0028	0.9056 \pm 0.0076	0.0642 \pm 0.0028	0.7951 \pm 0.0125	0.1381 \pm 0.0084
Probe + WV 16	0.8769 \pm 0.0058	0.1563 \pm 0.0079	0.8186 \pm 0.0121	0.1493 \pm 0.0183	0.8561 \pm 0.0069	0.1381 \pm 0.0149	0.8740 \pm 0.0177	0.0768 \pm 0.0069	0.8167 \pm 0.0049	0.1246 \pm 0.0197
MSV 1 + WV 16	0.8567 \pm 0.0130	0.1629 \pm 0.0074	0.8148 \pm 0.0113	0.1435 \pm 0.0071	0.8556 \pm 0.0067	0.1310 \pm 0.0074	0.9055 \pm 0.0075	0.0657 \pm 0.0028	0.7813 \pm 0.0039	0.1293 \pm 0.0082
MSV 16	0.9037\pm0.0201	0.1104\pm0.0105	0.8946\pm0.0229	0.1054\pm0.0076	0.9105\pm0.0115	0.1041\pm0.0049	0.9532\pm0.0069	0.0375\pm0.0029	0.8591\pm0.0029	0.1100\pm0.0063
Probe	0.8690 \pm 0.0135	0.1592 \pm 0.0101	0.8317 \pm 0.0089	0.1478 \pm 0.0232	0.8621 \pm 0.0108	0.1413 \pm 0.0195	0.9120 \pm 0.0141	0.0796 \pm 0.0105	0.8229 \pm 0.0142	0.1527 \pm 0.0242
MSV 1	0.8443 \pm 0.0223	0.1601 \pm 0.0125	0.8169 \pm 0.0135	0.1425 \pm 0.0076	0.8546 \pm 0.0104	0.1343 \pm 0.0028	0.9056 \pm 0.0076	0.0642 \pm 0.0028	0.7951 \pm 0.0125	0.1381 \pm 0.0084
Probe + WV 64	0.8769 \pm 0.0058	0.1563 \pm 0.0079	0.8186 \pm 0.0121	0.1493 \pm 0.0183	0.8561 \pm 0.0069	0.1381 \pm 0.0149	0.8740 \pm 0.0177	0.0768 \pm 0.0069	0.8167 \pm 0.0049	0.1246\pm0.0197
MSV 1 + WV 64	0.8567 \pm 0.0130	0.1629 \pm 0.0074	0.8148 \pm 0.0113	0.1435 \pm 0.0071	0.8556 \pm 0.0067	0.1310 \pm 0.0074	0.9055 \pm 0.0075	0.0657 \pm 0.0028	0.7813 \pm 0.0039	0.1293 \pm 0.0082
MSV 64	0.9128\pm0.0125	0.1147\pm0.0022	0.8879\pm0.0136	0.1072\pm0.0118	0.8953\pm0.0034	0.1173\pm0.0033	0.9648\pm0.0016	0.0323\pm0.0013	0.8352\pm0.0084	0.1255 \pm 0.0051

Table 28. ECE and NLL of verifiers trained and evaluated on streaming answers.

	MATH		OlympiadBench		AMC12		AIME		Omni-MATH	
	ECE \downarrow	NLL \downarrow								
Probe	0.0934 \pm 0.0416	0.5184 \pm 0.0528	0.1317 \pm 0.0382	0.5206 \pm 0.0914	0.1292 \pm 0.0461	0.4841 \pm 0.0689	0.0901 \pm 0.0384	0.2781 \pm 0.0415	0.1656 \pm 0.0470	0.5194 \pm 0.0945
MSV 1	0.0939 \pm 0.0163	0.5356 \pm 0.0441	0.0911 \pm 0.0163	0.5055 \pm 0.0208	0.0862 \pm 0.0164	0.4532 \pm 0.0039	0.0511 \pm 0.0229	0.2412 \pm 0.0113	0.1157 \pm 0.0132	0.4974 \pm 0.0232
Probe	0.0934 \pm 0.0416	0.5184 \pm 0.0528	0.1317 \pm 0.0382	0.5206 \pm 0.0914	0.1292 \pm 0.0461	0.4841 \pm 0.0689	0.1160 \pm 0.0385	0.2847 \pm 0.0421	0.1656 \pm 0.0470	0.5194 \pm 0.0945
MSV 1	0.0939 \pm 0.0163	0.5356 \pm 0.0441	0.0911 \pm 0.0163	0.5055 \pm 0.0208	0.0862 \pm 0.0164	0.4532 \pm 0.0039	0.0511 \pm 0.0229	0.2412 \pm 0.0113	0.1157 \pm 0.0132	0.4974 \pm 0.0232
Probe + WV 4	0.1052 \pm 0.0353	0.4842 \pm 0.0382	0.1817 \pm 0.0347	0.4885 \pm 0.0544	0.1272 \pm 0.0413	0.4410 \pm 0.0489	0.0861 \pm 0.0425	0.2784 \pm 0.0348	0.1104 \pm 0.0381	0.4407 \pm 0.0664
MSV 1 + WV 4	0.0822 \pm 0.0132	0.5204 \pm 0.0321	0.1292 \pm 0.0200	0.4836 \pm 0.0315	0.0767 \pm 0.0141	0.4272 \pm 0.0175	0.0548 \pm 0.0249	0.2447 \pm 0.0113	0.1030 \pm 0.0152	0.4550 \pm 0.0223
MSV 4	0.0814\pm0.0133	0.4637\pm0.0294	0.0797\pm0.0143	0.4289\pm0.0270	0.0638\pm0.0093	0.3709\pm0.0172	0.0271\pm0.0120	0.1814\pm0.0187	0.0959\pm0.0116	0.4206\pm0.0287
Probe	0.0934 \pm 0.0416	0.5184 \pm 0.0528	0.1317 \pm 0.0382	0.5206 \pm 0.0914	0.1292 \pm 0.0461	0.4841 \pm 0.0689	0.1160 \pm 0.0385	0.2847 \pm 0.0421	0.1656 \pm 0.0470	0.5194 \pm 0.0945
MSV 1	0.0939 \pm 0.0163	0.5356 \pm 0.0441	0.0911 \pm 0.0163	0.5055 \pm 0.0208	0.0862 \pm 0.0164	0.4532 \pm 0.0039	0.0511 \pm 0.0229	0.2412 \pm 0.0113	0.1157 \pm 0.0132	0.4974 \pm 0.0232
Probe + WV 16	0.1052 \pm 0.0353	0.4842 \pm 0.0382	0.1817 \pm 0.0347	0.4885 \pm 0.0544	0.1272 \pm 0.0413	0.4410 \pm 0.0489	0.0861 \pm 0.0425	0.2784 \pm 0.0348	0.1104 \pm 0.0381	0.4407 \pm 0.0664
MSV 1 + WV 16	0.0822 \pm 0.0132	0.5204 \pm 0.0321	0.1292 \pm 0.0200	0.4836 \pm 0.0315	0.0767 \pm 0.0141	0.4272 \pm 0.0175	0.0548 \pm 0.0249	0.2447 \pm 0.0113	0.1030 \pm 0.0152	0.4550 \pm 0.0223
MSV 16	0.0666\pm0.0211	0.3781\pm0.0461	0.0606\pm0.0166	0.3546\pm0.0195	0.0563\pm0.0108	0.3672\pm0.0173	0.0333\pm0.0146	0.1498\pm0.0109	0.0883\pm0.0122	0.3888\pm0.0163
Probe	0.0934 \pm 0.0416	0.5184 \pm 0.0528	0.1317 \pm 0.0382	0.5206 \pm 0.0914	0.1292 \pm 0.0461	0.4841 \pm 0.0689	0.1160 \pm 0.0385	0.2847 \pm 0.0421	0.1656 \pm 0.0470	0.5194 \pm 0.0945
MSV 1	0.0939 \pm 0.0163	0.5356 \pm 0.0441	0.0911 \pm 0.0163	0.5055 \pm 0.0208	0.0862 \pm 0.0164	0.4532 \pm 0.0039	0.0511 \pm 0.0229	0.2412 \pm 0.0113	0.1157 \pm 0.0132	0.4974 \pm 0.0232
Probe + WV 64	0.1052 \pm 0.0353	0.4842 \pm 0.0382	0.1817 \pm 0.0347	0.4885 \pm 0.0544	0.1272 \pm 0.0413	0.4410 \pm 0.0489	0.0861 \pm 0.0425	0.2784 \pm 0.0348	0.1104 \pm 0.0381	0.4407 \pm 0.0664
MSV 1 + WV 64	0.0822\pm0.0132	0.5204 \pm 0.0321	0.1292 \pm 0.0200	0.4836 \pm 0.0315	0.0767\pm0.0141	0.4272\pm0.0175	0.0548 \pm 0.0249	0.2447 \pm 0.0113	0.1030\pm0.0152	0.4550 \pm 0.0223
MSV 64	0.0913 \pm 0.0151	0.4135\pm0.0322	0.0868\pm0.0236	0.3770\pm0.0346	0.1054 \pm 0.0065	0.4293 \pm 0.0210	0.0165\pm0.0048	0.1254\pm0.0027	0.1316 \pm 0.0069	0.4296\pm0.0284

Parallel Test-Time Scaling with Multi-Sequence Verifiers

Table 29. Area Under the Tradeoff Curve (AUTC) of verifiers trained and evaluated on streaming answers.

	MATH	OlympiadBench	AMC12	AIME	Omni-MATH
Probe	1515.60 \pm 4.54	1018.33 \pm 5.09	924.22 \pm 13.90	563.44 \pm 19.34	651.90 \pm 6.05
MSV 1	1508.67 \pm 4.09	1007.82 \pm 7.29	928.82 \pm 10.99	551.56 \pm 7.02	652.47 \pm 3.12
Probe	2087.71 \pm 12.33	1276.03 \pm 27.60	1258.18 \pm 12.87	823.84 \pm 30.63	806.11 \pm 7.02
MSV 1	2030.51 \pm 6.77	1221.71 \pm 19.33	1245.30 \pm 11.16	793.35 \pm 15.39	787.05 \pm 10.14
Probe + WV 4	2074.56 \pm 11.23	798.03 \pm 13.92	1232.06 \pm 17.58	808.66 \pm 38.60	790.69 \pm 7.91
MSV 1 + WV 4	2034.65 \pm 5.09	1220.65 \pm 14.54	1247.01 \pm 14.53	789.28 \pm 17.55	780.09 \pm 6.47
MSV 4	2118.07\pm8.79	1282.20\pm19.29	1297.64\pm16.58	850.44\pm8.78	827.07\pm11.08
Probe	2397.75 \pm 10.97	1415.54 \pm 20.32	1457.76 \pm 13.37	1024.18 \pm 32.74	913.78 \pm 9.61
MSV 1	2293.65 \pm 29.83	1318.59 \pm 30.63	1421.14 \pm 24.60	954.76 \pm 26.23	870.03 \pm 5.86
Probe + WV 16	2387.20 \pm 22.08	1395.88 \pm 17.53	1412.28 \pm 20.37	1000.25 \pm 32.17	899.39 \pm 9.63
MSV 1 + WV 16	2280.68 \pm 17.58	1286.12 \pm 20.30	1432.93 \pm 27.27	959.76 \pm 28.52	860.55 \pm 6.27
MSV 16	2473.59\pm12.96	1460.66\pm22.79	1475.91\pm21.36	1078.29\pm18.00	948.81\pm10.43
Probe	2542.46 \pm 16.92	1481.58 \pm 26.21	1545.22 \pm 19.38	1149.40 \pm 32.65	1025.29 \pm 10.51
MSV 1	2292.01 \pm 46.51	1275.93 \pm 28.53	1423.86 \pm 47.98	1005.34 \pm 34.33	901.56 \pm 22.01
Probe + WV 64	2554.70 \pm 8.52	1464.85 \pm 22.84	1503.08 \pm 27.02	1167.81 \pm 40.73	973.23 \pm 12.37
MSV 1 + WV 64	2347.04 \pm 26.68	1287.00 \pm 22.95	1435.32 \pm 33.72	1045.05 \pm 40.58	903.09 \pm 20.84
MSV 64	2677.20\pm22.41	1551.33\pm46.96	1606.40\pm32.74	1289.80\pm15.48	1046.36\pm20.24

Table 30. AUROC and Brier score of training-free baseline methods for terminal answers.

	MATH		OlympiadBench		AMC12		AIME		Omni-MATH	
	AUROC \uparrow	Brier \downarrow								
Token Probs	0.5320	0.2504	0.7704	0.3696	0.7350	0.3540	0.8999	0.3073	0.7814	0.4467
Token Probs	0.5320	0.2504	0.7704	0.3696	0.7350	0.3540	0.8999	0.3073	0.7814	0.4467
Token Probs + WV 4	0.7922	0.1678	0.8392	0.2166	0.7978	0.2448	0.8223	0.2239	0.8085	0.2620
Self-consistency 4	0.7876	0.1686	0.8290	0.2180	0.7893	0.2477	0.8001	0.2274	0.7986	0.2627
Token Probs	0.5320	0.2504	0.7704	0.3696	0.7350	0.3540	0.8999	0.3073	0.7814	0.4467
Token Probs + WV 16	0.8155	0.1474	0.8801	0.1690	0.8364	0.1961	0.8531	0.1662	0.8457	0.1968
Self-consistency 16	0.8149	0.1482	0.8751	0.1704	0.8299	0.1991	0.8422	0.1696	0.8398	0.1976
Token Probs	0.5320	0.2504	0.7704	0.3696	0.7350	0.3540	0.8999	0.3073	0.7814	0.4467
Token Probs + WV 64	0.8304	0.1432	0.8901	0.1591	0.8454	0.1871	0.8608	0.1549	0.8531	0.1841
Self-consistency 64	0.8273	0.1440	0.8875	0.1605	0.8410	0.1900	0.8517	0.1583	0.8505	0.1849

Table 31. ECE and NLL of training-free baseline methods for terminal answers.

	MATH		OlympiadBench		AMC12		AIME		Omni-MATH	
	ECE \downarrow	NLL \downarrow								
Token Probs	0.1855	0.9190	0.4124	1.1444	0.3935	1.1384	0.4198	0.8669	0.5389	1.2505
Token Probs + WV 4	0.1615	1.1805	0.2416	1.2018	0.2616	1.4551	0.2677	1.1803	0.3306	1.4633
Self-consistency 4	0.1611	1.1823	0.2408	1.2054	0.2601	1.4620	0.2664	1.1889	0.3300	1.4647
Token Probs + WV 16	0.1212	0.9249	0.1566	0.6566	0.1752	0.8604	0.1545	0.6618	0.2235	0.8289
Self-consistency 16	0.1204	0.9264	0.1551	0.6605	0.1737	0.8673	0.1517	0.6702	0.2226	0.8306
Token Probs + WV 64	0.1158	0.7592	0.1346	0.5194	0.1549	0.7096	0.1254	0.5219	0.1970	0.6686
Self-consistency 64	0.1149	0.7598	0.1329	0.5231	0.1531	0.7161	0.1221	0.5301	0.1959	0.6692

Table 32. Best-of- N accuracy (ACC) with training-free baseline methods at $N = 1, 4, 16, 64$.

N	Method	MATH	OlympiadBench	AMC12	AIME	Omni-MATH
1	Token Probs	0.6755	0.4105	0.3965	0.2748	0.2432
4	Token Probs	0.6943	0.4495	0.4445	0.3313	0.2667
	Token Probs + WV 4	0.7102	0.4590	0.4450	0.3410	0.2723
	Self-consistency 4	0.7049	0.4484	0.4286	0.3251	0.2633
16	Token Probs	0.6959	0.4754	0.4664	0.3772	0.2835
	Token Probs + WV 16	0.7221	0.4788	0.4683	0.3711	0.2835
	Self-consistency 16	0.7210	0.4676	0.4478	0.3566	0.2801
64	Token Probs	0.7098	0.4978	0.5224	0.4129	0.3013
	Token Probs + WV 64	0.7299	0.4888	0.4627	0.3728	0.2902
	Self-consistency 64	0.7321	0.4844	0.4403	0.3594	0.2790

 Table 33. ECE and Brier score of confidence output on best-of N answers with training-free baseline methods at $N = 1, 4, 16, 64$.

N	Method	MATH		OlympiadBench		AMC12		AIME		Omni-MATH	
		ECE ↓	Brier ↓								
1	Token Probs	0.1855	0.5007	0.4124	0.7393	0.3935	0.7081	0.4198	0.6146	0.5389	0.8933
4	Token Probs	0.2157	0.5126	0.4320	0.7905	0.4109	0.7549	0.4447	0.6956	0.5775	1.0020
	Token Probs + WV 4	0.1588	0.3661	0.2549	0.5065	0.2763	0.5557	0.2789	0.5421	0.3698	0.6127
	Self-consistency 4	0.1613	0.3638	0.2586	0.4983	0.2843	0.5504	0.2805	0.5316	0.3708	0.6031
16	Token Probs	0.2517	0.5414	0.4480	0.8347	0.4372	0.8027	0.4599	0.7566	0.6065	1.0912
	Token Probs + WV 16	0.1296	0.3381	0.1907	0.4404	0.2094	0.4898	0.1849	0.4595	0.2952	0.5031
	Self-consistency 16	0.1292	0.3404	0.1971	0.4347	0.2235	0.4840	0.1927	0.4558	0.2961	0.5021
64	Token Probs	0.2653	0.5416	0.4556	0.8656	0.4143	0.7896	0.4757	0.8202	0.6271	1.1669
	Token Probs + WV 64	0.1305	0.3318	0.1670	0.4248	0.2075	0.4640	0.1663	0.4364	0.2742	0.4855
	Self-consistency 64	0.1259	0.3377	0.1680	0.4279	0.2196	0.4502	0.1733	0.4341	0.2830	0.4749

Table 34. AUROC and Brier score of training-free baseline methods on streaming answers.

	MATH		OlympiadBench		AMC12		AIME		Omni-MATH	
	AUROC ↑	Brier ↓								
Token Probs	0.7910	0.3399	0.8091	0.4266	0.7856	0.3979	0.8858	0.3217	0.7974	0.4746
Token Probs	0.7910	0.3399	0.8091	0.4266	0.7856	0.3979	0.8858	0.3217	0.7974	0.4746
Token Probs + WV 4	0.7867	0.3341	0.8028	0.4149	0.7774	0.3892	0.8784	0.3107	0.7889	0.4609
Self-consistency 4	0.5000	0.2500								
Token Probs	0.7910	0.3399	0.8091	0.4266	0.7856	0.3979	0.8858	0.3217	0.7974	0.4746
Token Probs + WV 16	0.7867	0.3341	0.8028	0.4149	0.7774	0.3892	0.8784	0.3107	0.7889	0.4609
Self-consistency 16	0.5000	0.2500								
Token Probs	0.7910	0.3399	0.8091	0.4266	0.7856	0.3979	0.8858	0.3217	0.7974	0.4746
Token Probs + WV 64	0.7867	0.3341	0.8028	0.4149	0.7774	0.3892	0.8784	0.3107	0.7889	0.4609
Self-consistency 64	0.5000	0.2500								

Table 35. ECE and NLL of training-free baseline methods on streaming answers.

	MATH		OlympiadBench		AMC12		AIME		Omni-MATH	
	ECE ↓	NLL ↓	ECE ↓	NLL ↓	ECE ↓	NLL ↓	ECE ↓	NLL ↓	ECE ↓	NLL ↓
Token Probs	0.3732	1.1043	0.5255	1.1625	0.4944	1.1466	0.4886	0.8724	0.6045	1.2632
Token Probs	0.3732	1.1043	0.5255	1.1625	0.4944	1.1466	0.4886	0.8724	0.6045	1.2632
Token Probs + WV 4	0.3644	1.0481	0.5135	1.1115	0.4840	1.0962	0.4757	0.8341	0.5929	1.2095
Self-consistency 4	0.0226	0.6931	0.2553	0.6931	0.2529	0.6931	0.3683	0.6931	0.3533	0.6931
Token Probs	0.3732	1.1043	0.5255	1.1625	0.4944	1.1466	0.4886	0.8724	0.6045	1.2632
Token Probs + WV 16	0.3644	1.0481	0.5135	1.1115	0.4840	1.0962	0.4757	0.8341	0.5929	1.2095
Self-consistency 16	0.0226	0.6931	0.2553	0.6931	0.2529	0.6931	0.3683	0.6931	0.3533	0.6931
Token Probs	0.3732	1.1043	0.5255	1.1625	0.4944	1.1466	0.4886	0.8724	0.6045	1.2632
Token Probs + WV 64	0.3644	1.0481	0.5135	1.1115	0.4840	1.0962	0.4757	0.8341	0.5929	1.2095
Self-consistency 64	0.0226	0.6931	0.2553	0.6931	0.2529	0.6931	0.3683	0.6931	0.3533	0.6931

Table 36. Area Under the Tradeoff Curve (AUTC) of training-free baseline methods.

	MATH	OlympiadBench	AMC12	AIME	Omni-MATH
Token Probs	1246.1625	874.4062	780.8859	423.6729	597.4429
Token Probs	1315.0728	804.3277	706.4964	353.0816	574.9029
Token Probs + WV 4	1341.3023	793.8698	721.3110	354.8151	572.9540
Self-consistency 4	1560.7934	944.5491	861.8922	550.2739	655.1951
Token Probs	1085.6131	712.8956	629.6273	322.1713	551.7789
Token Probs + WV 16	1120.1693	699.5992	649.8307	358.4021	555.1394
Self-consistency 16	1628.0505	960.6178	879.9306	565.9113	660.7702
Token Probs	836.6923	665.0830	557.9867	298.3862	532.7231
Token Probs + WV 64	869.1815	670.9667	609.4350	321.8818	526.9107
Self-consistency 64	1665.4385	998.9186	925.0327	545.8705	652.2426